



Review

Review of indium-free, transparent and flexible metallic fibers for wearable electronics



Bhavana Joshi^{a,1}, Edmund Samuel^{b,1}, Seongpil An^{c,1}, Siwung Kim^a, Alexander L. Yarin^{a,d,*}, Sam S. Yoon^{a,*}

^a School of Mechanical Engineering, Korea University, Seoul 02841, Republic of Korea

^b Energy Environment Policy and Technology, Graduate School of Energy and Environment (KUKIST Green School), Korea University, Seoul 02841, Republic of Korea

^c SKKU Advanced Institute of Nanotechnology (SAINT) and Department of Nano Engineering, Sungkyunkwan University (SKKU), Suwon 16419, Republic of Korea

^d Department of Mechanical and Industrial Engineering, University of Illinois at Chicago, 842 W. Taylor St., Chicago, IL 60607-7022, USA

ARTICLE INFO

Keywords:

Electrospinning
Electroplating
Electroless plating
Transparent metallic fibers
Transparent conductive electrode
Sputtering

ABSTRACT

The use of transparent metallic fibers (TMFs) in various applications, including touchscreens, solar cells, and transparent heaters, is gradually increasing, thereby emerging as a state-of-the-art technology in advanced portable and self-powered wearable electronics. This review discusses several novel approaches for fabricating TMFs that exhibit excellent transparency, flexibility, and low sheet resistance. TMFs are aimed to meet the increasing demand for soft and wearable electronic and optoelectronic devices. Lightweight and flexible TMFs are alternatives to indium tin oxide, which is expensive, brittle, and possesses low optical transmittance in near-infrared spectra. Moreover, TMF fabrication is scalable. This review focuses on crucial techniques employed in the fabrication of metallic fibers and presents key parameters in a tabular format. In addition, the insights of developing high-performance TMFs for various applications are provided. Finally, challenges associated with the fabrication and integration of TMFs in practical applications are discussed and addressed.

1. Introduction

Flexible and wearable electronic devices have attracted considerable attention because of their low weight, geometrical versatility, and integration into next-generation technologies. For instance, smart clothing [1], flexible touch displays [2], electronic skins [3], touchscreen sensors, and transparent heaters [4] are rapidly emerging as cutting-edge applications [5–7]. Metallic fibers and wires have been used to improve the adaptability and flexibility of human–machine interfaces (HMIs) and their endurance under bending, compression, or twisting, thereby contributing to the realization of aesthetic wearable electronic devices. According to IDTechEx, the popularity of smart wearables will drive the flexible electronic device market to be worth US \$74 billion by 2025 [8].

Flexible and robust conductive electrodes facilitate the integration of electronic devices into smart wearable devices [9,10]. Various conductive materials, such as graphene, carbon nanotubes (CNT), metal grids, silver nanowires, and conducting polymers, have been explored to achieve low sheet resistance (R_{sh}) in the electrodes [11–15]. However,

these conductive materials typically possess a low aspect ratio and high junction resistances, which limit their ability to replace brittle and less abundant indium tin oxide (ITO). Therefore, ITO remains the first choice for applications such as photovoltaics, smart windows, and de-icing heaters owing to its excellent conductivity [4,16]. In parallel, free-standing and flexible metallic fibers are emerging rapidly because of their superior flexibility, high aspect ratio, and low junction resistance, which make them compatible with flexible electronics and conformable with complex shaped objects, such as wearable devices [16].

Metallic fibers that reveal flexibility, low sheet resistance ($R_s < 5 \Omega \cdot \square^{-1}$), and high transparency ($T > 90\%$) are comparable to ITO or fluorine tin oxide in these applications. Specifically, transparent metallic fibers (TMFs), prepared by coating electrospun fibers with metals (Fig. 1) are increasingly being used as conductive electrodes in light-emitting diodes (LEDs) and solar cells.[17] The fabrication of conductive electrodes for wearable electronic devices uses electrospun fibers as templates and involves physical (e.g., physical vapor deposition, PVD) or chemical (e.g., electroplating, electroless plating) processes. PVD involves the evaporation or sputtering of solid metals to coat fibers with

* Corresponding authors at: School of Mechanical Engineering, Korea University, Seoul 02841, Republic of Korea (Sam S. Yoon).

E-mail addresses: ayarin@uic.edu (A.L. Yarin), skyoony@korea.ac.kr (S.S. Yoon).

¹ These authors equally contributed to this work.

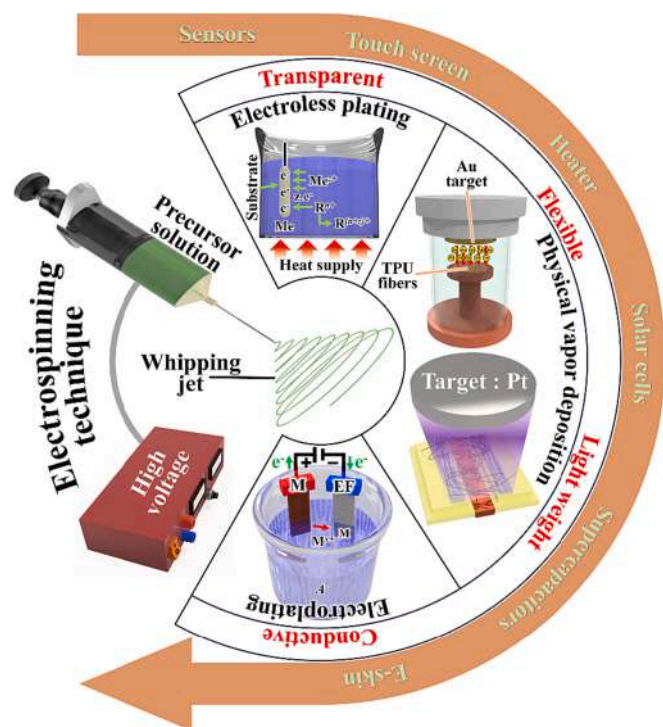


Fig. 1. Schematic illustrating compatibility of the electrospinning technique with various metal coating methods and their subsequent applications in wearable electronics.

metal [18–23]. In chemical processes, the conformal self-assembly of metallic cations helps create a nanotextured surface and can provide a wide range of surface structures, such as nanocones, thorny devils, and dendrites. Conversely, physical processes help derive smooth surface morphologies [24]. Wang *et al.* [16] suggested that chemical processes are more beneficial than physical ones for achieving scalability and realizing cost-effective conductive substrates. A recent comparison among various transparent electrodes (TEs) indicated that metal nanofibers and nanotroughs have a figure of merit of approximately 10 (on a scale of 1–10) [4]. However, metal nanofibers and nanowires have emerged as stronger TEs owing to their mechanical robustness. As bending strain decreases proportionally with thickness, thin metal nanofibers retain their superior mechanical strength and exhibit good fatigue resistance [4,16]. A freestanding transparent heater with low sheet resistance, which is capable of heating up to 280 °C at an applied potential of 1.5 V [16], was not discussed in the literature survey and investigation by Papanastasiou *et al.* [25]. Leote *et al.* [26] reviewed metalized polymer fibers for various electrochemical sensors; however, they did not discuss TMFs. Similarly, Yin *et al.* [27] and Chatterjee *et al.* [28] reviewed electromagnetic interference shielding and electronic textiles with nontransparent metal-coated flexible fibers without providing details of the fiber metallization process. These reviews indicate the potential of metalized fibers owing to their good conductivity. However, for solar cells, touch sensors, heaters, and smart windows, the fiber must possess high conductivity and transparency. This review discusses TMFs made from electrospun polymers with a metallic coating deployed using electroplating, electroless plating, or PVD. Section II covers the key parameters of the electrospinning and metallization processes to realize TMFs with improved characteristics. The main applications of TMFs, including heaters, solar cells, supercapacitors, touch screens, and wearable sensors, are discussed in Section III. This review discusses the state-of-the-art and future prospective applications of TMFs. Therefore, this review is expected to provide insights for the further development of TMFs and their integration into state-of-the-art technologies.

2. Electrospinning and fiber metallization techniques

The first studies on electrospinning dealt with cone-shaped water droplets (1600) and aerosols under the influence of an electric field (1740). Then, high-surface-to-volume viscoelastic polymer fibers were investigated (1887) [29,30]. A viscoelastic polymer solution under a controlled flow and high electric field strength transforms tiny cone jets into bending jet that leads to the formation of submicron fibers, which was first reported by Formhals (1934) [31]. Since then, the scalability of fiber production has increased considerably, as evident in the industrial production of gas mask filters (1950) and air filtration membranes (1980) [29]. Sun *et al.* [32] discussed the conditions for the formation of a Taylor cone (with an angle of 49.3°) and stable jet. Similarly, Yarin *et al.* investigated the physics, rheology, and tensile properties of electrospun polymer fibers [33–35].

Polymer electrospinning yields long fibers with high aspect ratios for various applications, such as drug delivery, tissue engineering, and energy storage devices [36,37]. The review of electrospun fibers for soft electronics indicates their flexibility, stretchability, conductivity, and transparency [38]. The post-processing of conductive fibers (e.g., annealing at high temperatures in an inert environment) has been widely reported. To achieve flexibility, conductivity, and transparency simultaneously, thin fibers (aligned or nonaligned) are fabricated and coated with metals using electroless plating [39–41], electrodeposition [42–44], and PVD [45]. These metallic fibers exhibit high transparency (>90%) and very low sheet resistance ($0.18 \Omega \cdot \square^{-1}$) [20].

Fig. 2 shows the electrospinning setup for the fabrication of free-standing fibers. A strong electrical field is required to draw the polymer fibers from a viscous solution [46]. Accordingly, the solvent, polymer concentration, and molecular weight are required to obtain a stable Taylor cone jet at the tip of the needle. The distance between the positive and negative electrodes of the applied electrical field can be tuned to obtain a stable Taylor cone jet; the high-speed camera image depicts the immediately stretched straight jet (Fig. 2). The jet experiences charge repulsion, causing a bending phenomenon (Fig. 2); subsequently, the fibers are collected on the grounded electrode.[47].

Ambient conditions during electrospinning, such as relative humidity and temperature, considerably affect the morphology and diameter of the fibers [38,48]. The relative humidity affects the evaporation of the solvent during formation of bending jet and can result in thinner fibers at lower humidity. However, reducing the humidity considerably can cause the breaking of fibers. Similarly, the fiber diameter can be tuned by controlling the ambient temperature [49]. This versatile electrospinning technique helps produce a wide range of fibers when an optimal polymer concentration is added to suitable solvents [46,50]. Further, the use of different structures of collectors impacts the preparation of aligned and nonaligned (nonwoven) fibers. A nonaligned electrospun nanofibers are collected onto the flat plate or a rotating drum when used as a grounded electrode. Conversely, the use of sharp grids, high-speed rotating drums, or conductive copper wire drums used as collector yields aligned fibers [51]. Such aligned and nonaligned fiber mats play an important role in pressure sensors [52], transparent conducting electrodes (TCEs) [16,53], and membranes [54].

Polymer-based transparent fibers exhibit very low electrical conductivities. Transparent fibers annealed at high temperatures are conductive but fragile. Therefore, metalized fibers or metallic fibers can be used as transparent conductive electrodes for various applications, such as touchscreens, sensors, e-skins [55,56], solar cells and heaters [57] (Table 1). Additionally, TMFs are lightweight, cost-effective, and flexible. Considering the benefits of TMFs, a few researchers have explored metallic nanotroughs by depositing electrospun fibers on metal films as masks, followed by the etching of unmasked metals and the removal of fibers. These metallic nanotroughs exhibit features similar to those of TMFs and, hence, are useful in the fabrication of organic light-emitting diodes and touchscreens.[58].

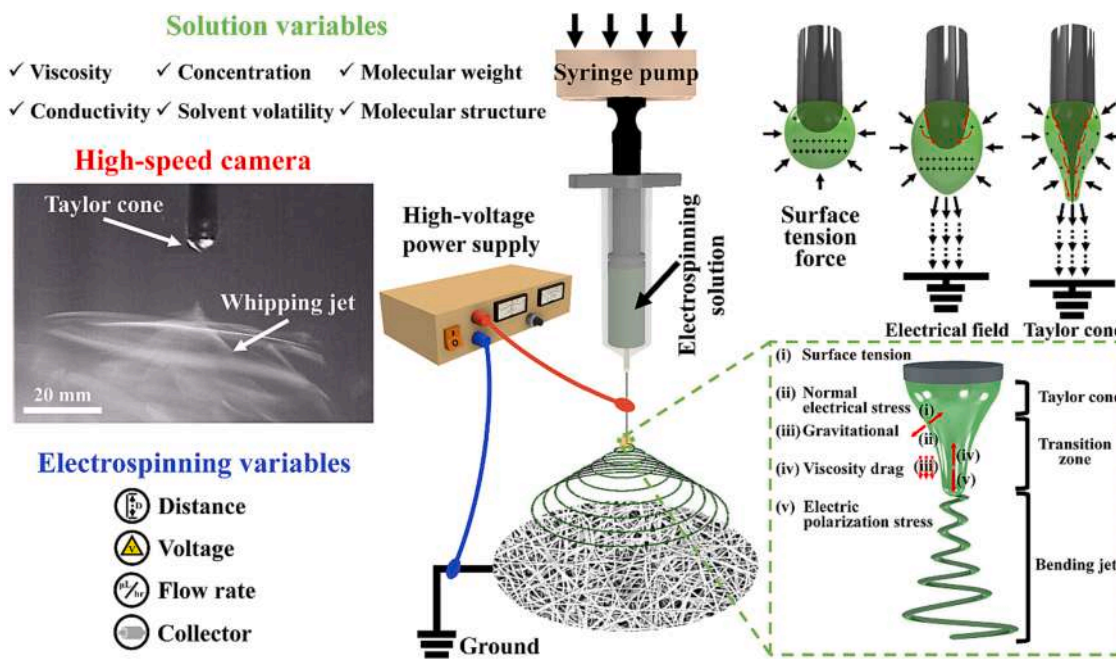
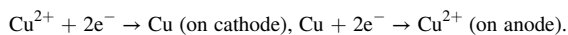


Fig. 2. Versatility of electrospinning, impact of electric field on droplets at needle tip, and a high-speed camera image depicting the formation of bending jet owing to change in surface charge, resulting in the transformation of the droplet to thin fibers at the collector.

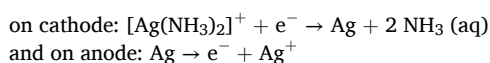
2.1. Metalized fibers via electroplating

Electroplating deposits a metal layer on conductive and semi-conductive substrates [59–61]. Metal deposition occurs because of the reduction in cations under an applied potential or constant current [59]. Semiconductive polymer fibers or non-conducting polymer fibers with a thin sputter-coated metal layer, which makes them conductive, are negatively biased to attract metal cations to electrolytes. A foil of a metal to be deposited onto the fibers is used as a positive electrode that provides metal cations *via* electrolyte during electroplating. The chemical process and reactions understanding are critical for achieving pure metallic coatings.

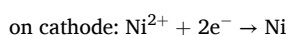
In particular, for electroplating of copper, sulfuric acid has to be added to the electroplating bath to facilitate conductivity and the process efficiency and minimize formation of the oxide layers. During the electroplating process, copper is dissolved at the anode with the help of sulfuric acid, while the copper anode reaches the solubility equilibrium with the dissolved CuSO_4 . On the other hand, copper is lost from the electrolyte during electroplating, while it deposits on nanofibers. The lost copper is simultaneously replaced by copper dissolved from the anode. Accordingly, the copper concentration in the electrolyte is constant during the electroplating process. It should be emphasized that not only Cu^{2+} , but also Cu^+ ions will be dissolved from the anode material [59]. The corresponding redox reactions take place on respective electrodes:



Similarly, for electroplating of silver the following reactions take place in the electroplating bath:

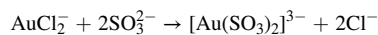
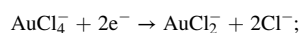


In brief, the redox reactions for nickel electroplating using nickel sulfamate, take place



and on anode: $\text{Ni} \rightarrow 2e^- + \text{Ni}^{2+}$

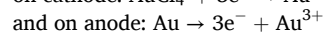
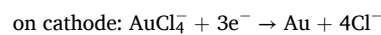
The gold electroplating reaction occurring in electroplating bath involves the following steps:



These correspond to the overall reaction:



and the following redox reactions,



As mentioned earlier, polymer fibers are sputtered with Pt/Au (Fig. 3) as a seed layer to make them semiconductive; this process is known as sensitization. Conversely, high-temperature inert-gas-pyrolyzed polymer fibers (e.g., carbon nanofiber [CNF]) can be used directly for metallization via electroplating (Adabi *et al.* [62] and Ercolano *et al.* [63]). However, depending on the electrospinning time, and annealing conditions, the fibers may or may not be transparent. Exceptional reports on the use of CNF as TMFs are available [64]. In these studies, non-plated fibers were removed by rinsing the metal-plated fibers in DMF to increase the transparency of the fibers [18,64].

Copper (Cu) [59,66–68], silver (Ag) [20], nickel (Ni) [18], gold (Au) [64], and platinum (Pt) [64] were electroplated using solutions of their respective metal salts (Table 2). Electrospun fibers were made semi-conductive using Pt (or Au) for the rapid metallization of the fibers by electroplating (Fig. 3a). The thickness of the metal coating on the electrospun fibers depends on the electrospinning and electroplating times. Moreover, the metal coating thickness depends on the metal salt concentration, applied current, or potential. The coatings of Ni, Pt, Au, Ag, and Cu were observed to entirely cover the electrospun fibers with distinct surface roughness (Fig. 3b).

Reports on copper electroplating suggest a wide range of surface

Table 1
Transparent metallic fibers as TCE in various applications.

Metal coating process	Material	Diameter (<i>D</i> , nm)	Sheet resistance (R_s , $\Omega \cdot \square^{-1}$)	Transmittance (<i>T</i> , %)	Mechanical stability		Application	Ref.
					Stretchability (%) and stretching cycle (at strain)	Bending cycle (radius)		
Electroplating	Cu	1320	0.340	76	580–770	1000 (5 mm)	TCE	[66]
Electroplating	Cu	1160–1190	0.370	96	300	1000 (1.3 mm)	Heater	[110]
Electroplating	Pt	1220	0.88	36	400 / 90 (200%)	2000	Water splitting	[64]
Electroplating	Cu	~ 1400	–	~ 90	–	3000 (0.7 or 3 cm)	Heater	[144]
Electroplating	Au	~ 1000	~ 2.7	~ 91	–	1000 (5 mm)	Heater	[64]
Electroplating	Ni	4750	0.73	93	300	2000	Heater	[75]
Electroplating	Cu	7280	0.18	93	–	–	Sensor	[19]
	Ni	10,400	0.31	93	–	–	–	–
Electroplating	Cu	3830	–	60	–	–	Air filter	[43]
Electroplating	Cu	2340	0.027	43	–	2000 (5 mm)	Air filter	[56]
Electroless plating	Al	50	120	95	–	–	–	[61]
Electroless plating	Cu	~ 200	11.2	91	–	1000 (4 mm)	TCEs	[89]
	Ag	–	8.5	90	–	–	–	–
Electroless plating	Ag	258	1.12	69	–	100 (5 mm)	TCEs	[76]
Electroless plating	Cu	100–2500	35	90	–	1000 (15 mm)	TCEs	[77]
Electroless plating	Cu/Ni	~ 160	~ 120	~ 88	–	100 (15 mm)	Heater	[2]
Electroless plating	Cu	~ 340	4.9	90	–	–	Heater	[75]
Electroless plating	Ag	600	40.3	81.4	–	500 (4 mm)	Flexible electrode	[22]
Electroless plating	Cu	–	40	90	–	1000 (5 mm)	Flexible transparent electrode	[79]
Sputtering	Pt	200–600	275	94	–	1000 (11 mm)	Dye-sensitized solar cell	[71]
Sputtering	CuZr	~ 200	18	98	15,000/ (70%)	–/ (0.004 mm)	Heater	[124]
Sputtering	Pt	260	400	98	160	–/ (1 mm)	TCE	[53]
Sputtering	Ag	700	1.4	91	–	2000	Hyperthermia patch	[55]
Magnetron Sputtering	W/Ag	1220	4.2	80	–	–	TCF	[98]
E-beam	Au	5100	24	98	–	100,000 (5 mm)	Organic solar cell	[127]
E-beam	Au	464	30	~ 91	–	–(1 mm)	Photodetectors	[103]
Thermal evaporation	Cu	–	25	~ 96	40	2000 (2 mm)	Heater	[96]
Thermal evaporation	Au/Cr	2300	8.2	84	70/1000	1000 (1.5 mm)	TCE	[122]
Thermal evaporation	Au	–	0.15	75	–	–	Stretchable interconnects	[120]
Thermal evaporation	Ag	–	2.4	94	–	10,000 (1 mm)	Organic solar cell	[17]
Thermal evaporation	Au	–	3	75	–	30,000 (1 mm)	Neural electrocorticogram	[56]

morphologies, depending on drying conditions. For instance, when Cu-plated nanofibers are dried in the air, it may result in oxidation, thereby forming thorny devil nanotexturing on the electrospun fiber surface [69]. Drying Cu-plated fibers in nitrogen (N_2) gas prevents the oxidation of the as-electroplated fibers and produces metal fibers with a rough morphology [66]. Thus, electroplated fibers must be carefully washed and dried to ensure high transparency and conductivity. Furthermore, the electrospinning and electroplating times need to be optimized to reduce junction resistances for the integration of the fibers in optoelectronic devices. Cu-electroplated nanofibers undergo oxidation when used as transparent heaters [19] or in electrochemical reactions [70] resulting in the irreversible degradation of Cu. Conversely, the oxidation of Ni-coated fibers is much slower (An *et al.* [18]); therefore, it can be used as a Cu-protective coating (Soram *et al.* [70] and Jo *et al.* [19]).

Pt, a noble metal, exhibits stable performance and excellent catalytic activity when used as a metal electrode. Thus, Pt is technologically important in fields, such as dye-sensitized solar cells (DSSCs) [71], photoelectrochemical (PEC) water splitting, sensors, and actuators [63]. However, Pt is expensive, and its availability is limited (concentration

0.4 ng g^{-1} on Earth) [72]. Similarly, gold is expensive but exhibits a high work function and excellent stability in extremely corrosive environments. Although Pt and Au have been coated on fibers via electroplating, their use is subject to strict feasibility checks and efficient use.

Nucleation and crystal growth during the electrodeposition of metals play a significant role in the development of nanotextured and rough/smooth morphologies. When the crystal growth rate is faster than that of nucleation, a rough metal surface is obtained. However, when the nucleation rate is greater than the crystal growth rate, electrodeposition results in a smooth metal coating. The nucleation and crystal growth rates can be tuned by controlling parameters, such as reactant concentration, temperature, and applied current density [59].

2.2. Metalized fibers via electroless plating

Electroless plating is a conformal coating technique that can be applied to conductive and nonconductive surfaces [76,77]. The solution chemistry in electroless plating can be used for the ultrathin coating of nanostructures [78,79]. This process preserves the physical and

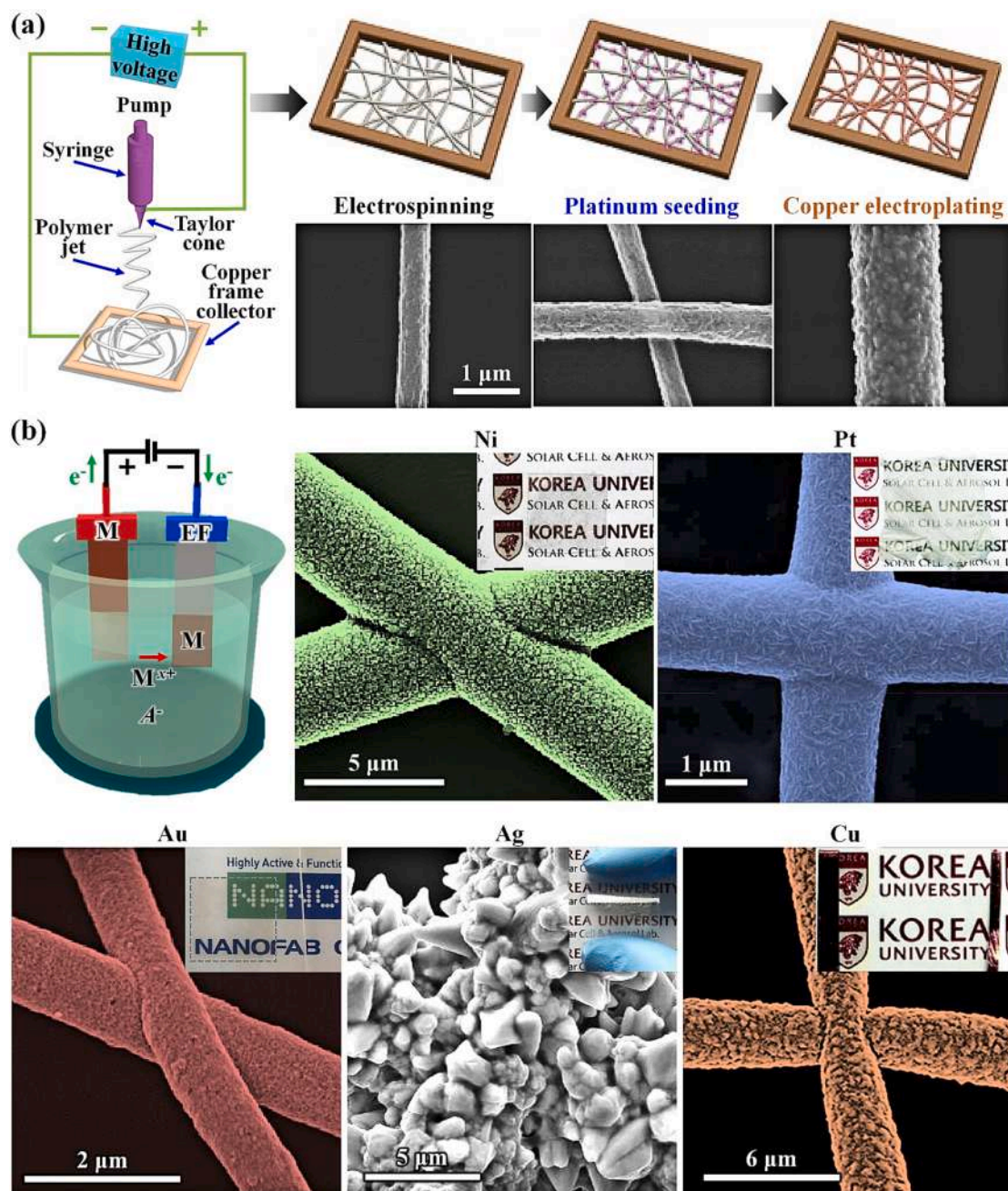


Fig. 3. (a) Electrospinning of polymer fibers and sensitization via sputtering (metal seeding), followed by electroplating to produce metallic fibers. Reproduced from [42,65] ©2016 Elsevier and ©2017 Springer Nature. (b) Electroplating process using electrospun fibers (EF) and scanning electron microscopic (SEM) images exhibiting the nanotextured surface of fibers electroplated with nickel [18] (©2018 Elsevier), platinum [64] (2017 © permission conveyed through Copyright Clearance Center, Inc.), gold [64] (©2017 Elsevier), silver [20] (©2019 Elsevier), and copper [19] (2018 © permission conveyed through Copyright Clearance Center, Inc.). The inset shows the respective images of transparent metal fibers.

chemical characteristics of nanostructured templates. However, the surfaces of these templates need to be modified to ensure the conformal coating by electroless plating [80]. Less expensive metals, such as copper, cobalt, and nickel, or expensive metals, such as gold, palladium, platinum, and silver, can be efficiently coated on various polymers, such as polyester [81], polycaprolactone [82], poly(acrylonitrile) (PAN) [78], and polyaniline-based coagulates [83]. Polymers, metals, and reducing agents (formaldehyde and sodium borohydride) must be optimized to achieve the required characteristics, such as transmittance and sheet resistance.

Warren *et al.* [84] confirmed that nickel with relatively uniform and predetermined thickness can be obtained *via* electroless plating, whereas

PVD coatings varied owing to the shadowing effect of CNF. Considering their cost-effectiveness and lack of requirements for a conductive substrate, electroless plating techniques are promising. The deposited weight of the metal can be determined using Eq. (1) for nickel-coated fibers [85]. In this equation, γ , ρ_{Ni} , ρ_c , and G represent the fiber diameter, densities of Ni and carbon, and fiber weight, respectively. $\Delta\gamma$ represents the difference between the values obtained before and after the electroplating process.

$$\Delta\gamma = \left(\sqrt{1 + \frac{\rho_{Ni}}{\rho_c} \frac{\Delta G}{G}} - 1 \right) \gamma \quad (1)$$

Electroless plating techniques involve cleaning the fibers with

Table 2
Electroplating metal, electrolyte baths, electrodes, and current.

Metal	Electrolyte bath	Electrodes	Current/voltage (Plating time)	Morphology	Sensitized or carbonized fiber
Cu [66]	H ₂ SO ₄ , HCl, copper sulfate and formaldehyde	Cu and Pt/PAN/ Cu frame	3 V (3 s)	Rough	Pt sputter coating
Pt [64]	H ₂ PtCl ₆ pH ~1.5 H ₂ SO ₄	Pt plate and Pt/PAN/Pt frame	0.11 A cm ⁻² (15–90 min)	Nanotextured @45 min	Pt sputter coating
Ni [75]	(Ni(SO ₃ NH ₂) ₂ ·4H ₂ O, H ₃ BO ₃ , NaOH,	Ni foil and Pt/PAN/ Ni frame	0.22 A cm ⁻² (1 min)	Slight rough	Pt sputter coating
Ag [20]	potassium argentocyanide, and potassium cyanide and KS 700 (consisted of sodium borate, potassium phosphate, and phosphates)	Ag and Ni/Pt/PAN/ Ni frame	8 V (5 s)	Dendritic morphology	Pt sputter coating
Au [64]	Au electroplating solution	Pt and CNF/SUS frame	0.85–1 V (3 min)	Rough	Carbonized

acetone, followed by sensitization and activation. The pretreatment of the electrospun fibers roughens the surface, thus improving the metalization process and reducing the possibility of the flaking of the coated material. The fiber undergoes two steps of Sn–Pd catalyst seeding and

subsequently serves as a nucleus for electroless metal plating [78,86,87]. The sensitization and activation processes of the fibers are essential for realizing a conformal coating (Fig. 4a) [73,88]. The metal coating thickness depends on the metal ion concentration, reducing

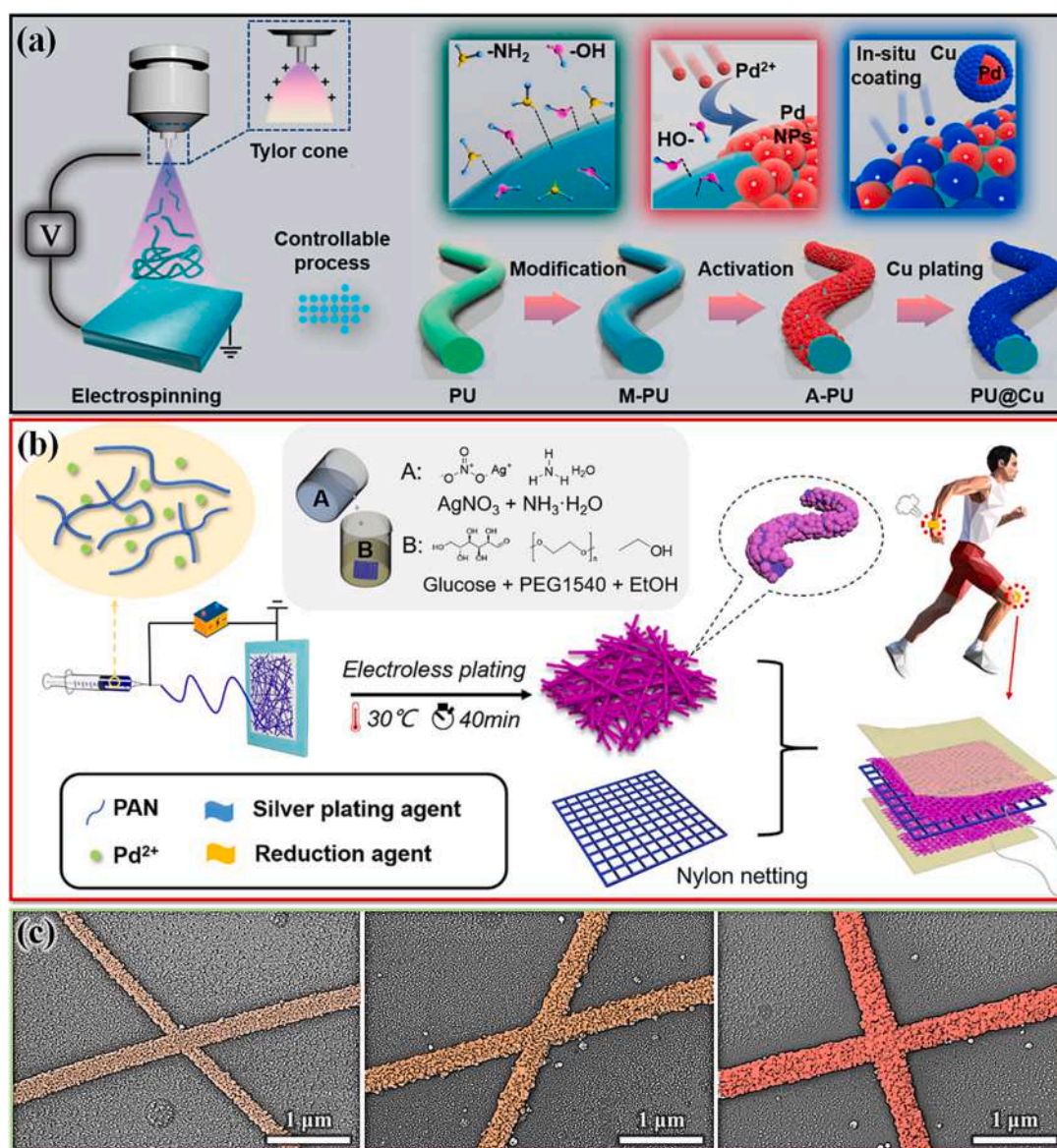


Fig. 4. (a) Surface activation and sensitization of fibers and electroless deposition of Cu on polyurethane fibers. Reprinted from [73] © 2021 American Chemical Society. (b) Pd-incorporated poly(acrylonitrile) nanofibers followed by silver coating via electroless plating for wearable pressure sensors. Reprinted from [74] ©2020 Elsevier. (c) SEM images showing flat copper nanofibers via electroless deposition for 2, 6, and 10 min on PdCl₄-seeded poly(vinylpyrrolidone)-derived fibers. Reproduced from [75] ©2018 Springer Nature.

agent, complexing agent, stabilizer, temperature, and pH of the electroless plating chemical solution [82,88,89].

A novel self-polymerization method using a polydopamine coating was introduced by Mondin *et al.* as a substrate-free activation process for electroless metallization on complex geometries [90]. The natural preference of polydopamine for metals and the pH of the electrolyte led to the effective deposition of novel metals for various applications, such as antibacterial coating or surface-enhanced Raman scattering (SERS) [90,91]. Recently, Xia *et al.* [73] reported the electroless plating of copper on electrospun polyurethane nanofibers (PU; Fig. 4a). They pretreated PU fibers using chitosan-PdCl₂. The chelate bonding of nitrogen from chitosan with Pd occurs because of the lone pair of electrons of nitrogen, resulting in uniform seeding for subsequent Cu plating. To further simplify the activation process, Chen *et al.* [74] fabricated electrospun PAN/PdCl₂ nanofibers and coated silver directly on the fibers using AgNO₃ and a glucose-polyethylene glycol electrolyte during electroless plating (Fig. 4b). Similarly, Kim *et al.* [75] prepared poly(vinylpyrrolidone) (PVP) fibers with (NH₄)₂PdCl₄, which was followed by heat treatment at 500 °C. Post-processing ensured the fusion of the polymer fiber junctions, and the PVP coating was removed over the PdCl₄ particles owing to the decomposition of PVP. Increasing the electroless deposition duration to 2, 6, and 10 min resulted in an increase in fiber diameters and Cu-coating thicknesses (Fig. 4c).

A literature survey suggests four major approaches for the pretreatment (sensitization and activation) of electrospun fibers for metallization. Sensitization and activation can be carried out by using SnCl₂ and PdCl₂, polydopamine and PdCl₂, spraying SnCl₂ on the fibers [92] and incorporating PdCl₂ directly into the electrospun polymer fibers. Among these approaches, SnCl₂ spraying is used for patterned metallization (Miao *et al.* [92]). Thus, the metallization of electrospun fibers using an electroless metal plating technique is promising for flexible optoelectronic devices [73].

2.3. Metalized fibers via sputtering and electron beam evaporation

PVD is beneficial for spontaneously depositing metal onto electrospun fibers without any prerequisite of conductivity or sensitization/activation of the fiber surface. In evaporation-based PVD, the metal source melts via resistive heating or electron beam systems and is then deposited on the fiber [96]. During sputtering, the ions of the noble gas plasma eject the source metal by bombardment, generating a stream of source ions toward the substrate. Direct current (DC) or magnetron sputtering is the preferred method for metal deposition [97,98]. Thus, this technique is widely used for industrial manufacturing, specifically in solar cells, wearable electronics, and commercial displays [99]. Metal deposition by evaporation or sputtering requires a vacuum region to achieve high efficiency and a high deposition rate (1 to few hundred nanometers per second) [24,100]. Metal deposition is performed on both sides of the fiber to reduce shadowing effects and obtain a uniform metal coating. Modern PVD systems with a substrate rotation function considerably improve coating uniformity [101]. However, thick fibers may still suffer from shadowing effects because PVD technology is based on the line-of-sight principle [24].

Despite the advantages of the PVD technique, it has a minor drawback with regard to the preservation of the biocompatibility of electrospun fibers. The deposition rate or plasma treatment time during sputtering must be optimal for biopolymer fibers to avoid the irreversible destruction of the scaffold surface based on the radiation flux of the plasma discharge [102]. These methods are used to produce nonconductive fibers partially conductive before electroplating and deposit metal fibers with various nanostructures (nanocoils, thorny devils, and so on) [20,66]. Conversely, the morphology of the fibers after metal deposition by PVD remains uniform and smooth [58].

Chromium, gold, copper, silver, aluminum, platinum, and nickel can be coated on various electrospun fibers using electron beam evaporation (EBE) [103] and sputtering [58,93,95]. Chung *et al.* [93] sputtered SERS

active gold over thermoplastic polyurethane (Fig. 5a). They suggested that a lower fiber diameter is better and addition of HCl with polyurethane during electrospinning reduces the average diameter of fibers from 1048 to 231 nm. Thin and flexible sensors are wearable and suitable for the noninvasive detection of sweat-based analytes via SERS.

Fuh *et al.* [94] electrospun poly(vinylidene fluoride) (PVDF) fibers on a copper frame to reduce the fiber density, resulting in highly transparent electrodes (Fig. 5b). The PVDF fibers are stable during the sputtering process and can be used as a template to obtain TMFs with excellent conductivity. Pt-coated PVDF fibers can be encapsulated in polymethylsiloxane (PDMS), and such transparent and conductive templates exhibit high aspect ratios of 100,000 and 90% transmittance when the sheet resistance of TMF is 50 Ω·□⁻¹. Increasing the sputtering time reduced the sheet resistance and transmittance. Therefore, the sputtering time is critical for achieving a balance between transparency and conductivity.

The multiscale network of mesoscale Cu-coated fibers (diameter: 1–5 μm) and nanoscale Ag nanowire (AgNW) was reported by Hsu *et al.* as TCE for optoelectronic devices [95]. Traditionally, such multiscale combinations have been fabricated using lithography; however, the process is expensive and complex. In contrast, the complicated processes of lithography are reduced by transferring mesoscale wires of copper (CuMWs) onto AgNWs obtained through thermal evaporation of copper on electrospun polymer fibers. The electrospinning of the polymer was performed on floating electrodes to yield aligned electrospun fibers, following which the thermal evaporation of copper was performed to form freestanding and aligned CuMWs. The wire density and spacing control are more accessible in electrospinning than in lithography. The CuMWs then contacted the AgNWs using a roll press. Fig. 5c presents the fabrication and arrangement of a multiscale network. Here, the AgNWs are used to transport electrons for shorter distance (several hundreds of micrometers), and the mesoscale Cu fibers transport electrons across several millimeters. As a result, this multiscale network achieves higher conductance, low ohmic losses and higher transparency simultaneously. The SEM images show the combination of mesoscale particles and nanowires and the intersecting area. The versatility of this technique enables the application of the mesoscale nanowire concept in optoelectronic devices. The effectiveness of such a multiscale network was demonstrated by using it in an electrochromic device with poly(3,4-ethylenedioxythiophene) (PEDOT), which exhibited a coloration response time. The color appears to be light blue at +0.2 V and dark blue at -0.4 V (Fig. 5c). PVD and sputtering processes yield a thin coating of metals and are preferable for smoother surfaces of conductive electrodes.

Electrodeposition or electroplating of metals occurs on a conductive substrate, or nonconductive substrate with metallic seeding, under an applied potential or constant current. The time required for electroplating is significantly less than electrodeposition and this process can engineer the morphology of the layer based on application requirements. However, the metallic coatings are non-uniform and thickness control is challenging. By contrast, electroless plating can create uniform and conformal coating on three-dimensional templates, such as fibers, foams, or fabrics. This process is slower than electroplating because no applied potential or current is acting. Electroless plating faces the challenge of controlling the generation of pinholes owing to the appearance of hydrogen bubbles during the hydrogen evolution reaction (HER). This issue can be addressed by using the duplex coating approach to control hydrogen bubble generation and protect the electroplated film characteristics [104]. Sputtering and evaporation techniques also coat a thin layer of metal on a substrate, similar to the electroless plating process. However, these physical metal coating techniques are limited by adatom mobility and the shadowing effect, which causes non-uniformity in the fiber metallization [105]. Nevertheless, physical techniques provide good adhesion between the fiber template and the deposited material.

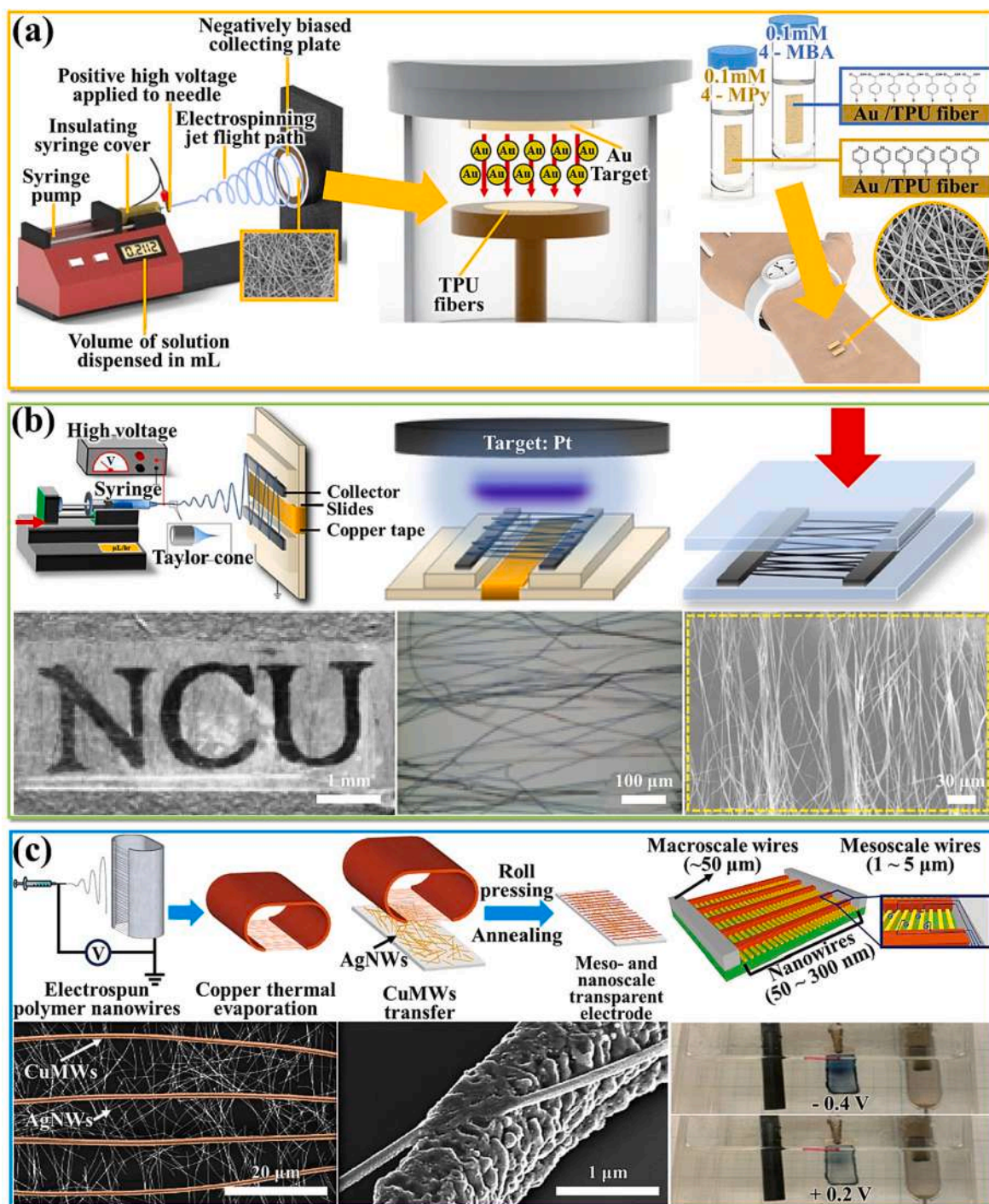


Fig. 5. (a) Health-monitoring device with gold-sputtered thermoplastic polyurethane electrospun fibers. Reprinted from [93] © 2021 American Chemical Society. (b) Pt-coated aligned poly(vinylidene fluoride) fibers, packaging, snapshot, and SEM images of TMFs. Used from [94] 2013 © permission conveyed through Copyright Clearance Center, Inc. Cu-coated PVP fibers produced via thermal evaporation and roll-pressed on the Ag nanowire (AgNW). The SEM images of the copper mesoscale wire (CuMW), underlying AgNW, and the fused junction (see high magnification). Utilization of CuMW/AgNW as TCE in an electrochromic device. Reprinted from [95] ©2013 Springer Nature.

3. Indium-free transparent metallic fiber applications

Metallic fibers are important in various applications owing to their excellent conductivity, high optical transmittance, flexibility, scalability, and cost-effectiveness. The optical and electrical properties of TMFs are fine-tuned to exceed the characteristics of well-known transparent conductive electrode materials, such as ITO [106] and fluorine-tin oxide [107]. Touchscreen displays and solar cells may require small-to-large

panels of TMFs, which can be readily fabricated using ultralong and continuous electrospun fibers. The TMFs must be stretchable and bendable for foldable mobiles, shatter-proof displays, wearable health-monitoring sensors, and flexible organic solar cells, which addresses the limitations of scarcely available indium and mechanically brittle ITO [2,108,109]. TMFs based on copper (price US \$6.36/kg and $\rho = 16.8 \text{ n}\Omega\text{-m}$) and silver (price US \$505/kg and $\rho = 15.9 \text{ n}\Omega\text{-m}$) appear to be more reasonable than those based on noble metals and ITO [108]. However,

TCEs fabricated using copper and silver nanowires via solution process techniques yielded $R_s = 40$ and $9 \Omega \cdot \square^{-1}$, respectively. [89] These sheet resistance values are much higher than those of silver ($R_s = 1.49 \Omega \cdot \square^{-1}$) [110] and copper fibers ($R_s = 0.06 \Omega \cdot \square^{-1}$) [65]. This explains an increasing interest in freestanding fibers and their metallization. This section highlights the use of TMFs in various electronic and energy applications.

3.1. Touchscreen sensors and displays

A touchscreen is an assembly of panels in an electronic device that, when touched, develops a net potential difference and subsequently causes charge flow between the electrodes. A touchscreen sensor refers to the response of a touchscreen when subjected to soft touch, acoustic

waves, or optical waves in conjunction with a sensing arrangement. The operation of a touchscreen fundamentally depends on the resistive or capacitive characteristics of the material and its design. Flexible touchscreens are emerging owing to the feasibility of manufacturing transparent junction-free metal fiber electrodes using electrospinning and metal deposition techniques [111,112]. The fabrication of scalable TMFs with an area of $33 \text{ cm} \times 21 \text{ cm}$ using magnetron sputtering and electrospinning has been demonstrated. Zhong *et al.* fabricated a touchscreen and organic light-emitting diode (OLED) to demonstrate the superior characteristics of TMF panels [112]. Touchscreen panels establish an HMI that eases the operation of soft robotics or health monitoring devices with a gentle touch or motion. Touchscreens can be designed for multi-touch or continuous touch (like scrolling). Accordingly, the driving, sensing, and bridge electrodes should be combined

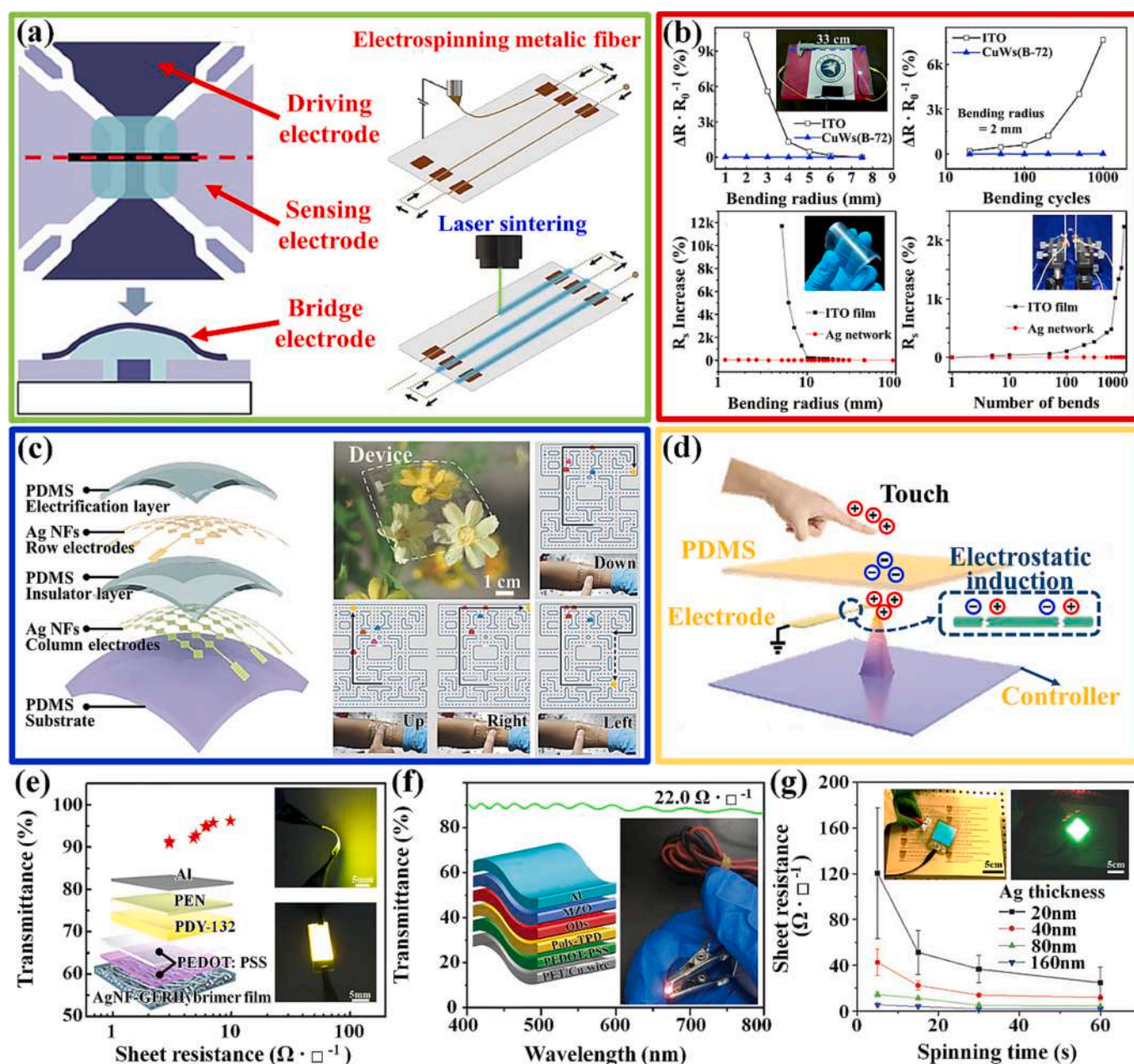


Fig. 6. TMF for a flexible touchscreen device: (a) near-field electrospinning of combined driving, sensing, and bridge electrodes. Reproduced from [113] ©2020, John Wiley and Sons. (b) Cu and Ag TMFs exhibiting excellent bending and transparent characteristics. Reprinted from [112,114] 2019 © permission conveyed through Copyright Clearance Center, Inc. and ©2015, American Chemical Society. (c) Touchscreen device assembly and Pac-Man demo. (d) Schematic of electrostatic field impact. Reprinted from [115] ©2018 Wiley-VCH. (e-g) OLED and QLED illumination images and characteristics. Adapted from [112,117,118].

(Fig. 6a). Thus, if sintering is required during the fabrication of a touchscreen, it must be performed carefully. Therefore, rapid and low-power laser sintering at specific locations or lines is preferred to preserve the remaining touchpad area (Fig. 6a) [113].

Wu *et al.* [58] fabricated a TMF using a thermal evaporation method. The fiber coating thickness of metals, such as copper, gold, and silver, was in the range of 80–100 nm to maintain the sheet resistances at 2, 8, and $10 \Omega \cdot \square^{-1}$, respectively. Additionally, a thin metalized fiber was needed to achieve 90% optical transmittance for touchscreen applications [58]. Metal nanotrough networks exhibit bendability with a radius of 2–100 mm without any increase in resistance [58]. Similarly, Cu nanotroughs with R_{sh} of $22 \Omega \cdot \square^{-1}$ and an Ag fiber network with R_{sh} of $7.6 \Omega \cdot \square^{-1}$ having a transmittance of ~91% exhibit excellent flexibility for approximately 1000 bending cycles (Fig. 6b and 6c) [112,114].

A touchscreen with low-resistive or low-capacitive features exhibits a rapid response time; consequently, touchpads for tactile sensing can enable state-of-the-art applications in the health industry [115]. Fig. 6d shows a touchscreen sensor with multiple layers of silver nanofibers sandwiched between the polymers. The Pac-Man images and snapshots of the touchscreen device demonstrate excellent sensing capability and transparency. Interestingly, both features of the silver fiber network matched well with those of PDMS. Additionally, PDMS can help improve the electrostatic field during contact electrification (CE) to tribo-electrification, that is, the convolution of the CE and charges due to friction. [116] Thus, integrated touchscreens for sensing devices have enabled the development of self-powered sensors. The operation of the device is explained briefly in Fig. 6d; charge flow occurs when a finger touches the PDMS. Consequently, induction current is generated below the silver fiber network layer (Fig. 6d) owing to the generation of an electrostatic field [115]. Thus, low-sheet-resistance TMFs in touchscreens have immense potential for integration in various applications. Moreover, the incorporation of TMF-based touchscreens with low sheet resistance reduces power consumption when integrated into health-monitoring systems, wireless communications, or fitness-tracking devices.

Flexible optoelectronic devices such as LEDs are becoming prominent for wearable smart displays [117]. Flexible devices can be assembled using all flexible components or integrated rigid and flexible components with stretchable interconnects [119,120]. Interestingly, Park *et al.* [117] reported all flexible layers of OLED using electrospinning-based Ag fiber networks prepared using terpineol and silver nanoparticles. Such AgNFs exhibited a low sheet resistance of $3 \Omega \cdot \square^{-1}$ and transmittance of 91% (Fig. 6e). An Ag-fiber-network-based TMF on a glass-fabric-reinforced hybrimer (GFRhybrimer) exhibited better bending stability than ITO-coated polyethylene terephthalate (PET). Furthermore, the Ag fiber network-based GFRhybrimer showed excellent thermal and corrosion stability. Thus, it, when used in OLEDs, exhibits a brightness of $59,918 \text{ cd} \cdot \text{m}^{-2}$ with an external quantum efficiency (EQE) of 4.6%. [117] Zhong *et al.* [112] used Cu nanotroughs with a PEDOT:PSS (polystyrene sulfonate) and quantum dots of CdSe/CdS/ZnS to fabricate quantum dot LEDs (QLEDs) (Fig. 6f). This QLED exhibited EQE of 2.9% and brightness of $1.9 \times 10^3 \text{ cd} \cdot \text{m}^{-2}$. Recently, Ciobotaru *et al.* [121] prepared electrospun fibers with a gold coating for use in OLEDs. However, the maximum transmittance value reported was ~70%, with a higher R_{sh} value of $7 \Omega \cdot \square^{-1}$. Choi *et al.* [118] reported 40 nm Ag coating fiber electrodes that exhibited a transmittance of ~92% and $R_{sh} = 22.3 \Omega \cdot \square^{-1}$ (Fig. 6g). When used with OLED, the maximum EQE was obtained to be 1.69%. Along with the R_{sh} values of the TMF, LEDs differ in terms of the material and layer thickness; therefore, the EQE cannot be directly compared. In addition to their flexible characteristics, stretchable electrodes require voids; however, a large number of voids reduces mechanical strength. Thus, Lee *et al.* proposed a hierarchical Au mesh comprising large and small voids forming a 2D web-in-web structure that provided superior stretchability for TCEs [122]. They used a top-down approach involving electrospinning and photolithography to fabricate web-in-web structures consisting of stretchable and

transparent conductors (STC). The diagonal alignment of the large voids delivers a stretchability of up to 70% without a change in the sheet resistance. The web-in-web Au network exhibits 84% transmittance at 550 nm with a sheet resistance of $8.2 \Omega \cdot \square^{-1}$. Thus, metal selection, fiber diameter, and the overall structure of TMFs are important for producing high transmittance and low R_{sh} values, which affect the optical properties of LEDs [121].

3.2. Transparent heaters

Transparent heaters are devices with electrically conductive layers that generate heat owing to the Joule effect when current flows through them. Transparent heaters are used as defrosters in automobile windows, flexible outdoor panel displays, and electronic devices that operate in extreme cold. Additionally, they can be attached to human clothes to keep the body warm, are portable, and can be operated with low-voltage batteries. These heaters are suitable for environments requiring temperature-controlled surfaces [18,25].

The important parameters of heating applications are transparency, sheet resistance, applied bias, and temperature generated by Joule heating. Jang *et al.* [125] used AgNF networks by directly electrospinning Ag nanoparticle/ethylene glycol ink as transparent heaters. The electrospun AgNFs were photoannealed using a xenon lamp for 30 min. The AgNF networks were transferred on PET to fabricate the transparent heater with $T = 83\%$ and $R_s = 0.5 \Omega \cdot \square^{-1}$. With an increase in voltage (V) to 4.5 V, the average temperature of the heater based on AgNF networks increased up to $249.5 \text{ }^\circ\text{C}$, and the saturated temperatures of heaters based on ITO ($R_s = 50 \Omega \cdot \square^{-1}$) and AgNW ($R_s = 10 \Omega \cdot \square^{-1}$), which exhibited the same transmittance ($T = 83\%$), merely increased to 29 and $54 \text{ }^\circ\text{C}$, respectively. This report demonstrates the large-scale fabrication of a heater with a size of $30 \times 30 \text{ cm}^2$ through a roll-based electrospinning system and the wireless operation of a heater for smart living.

The high-purity Ni-electroplated NF that bonded the fibers at their junctions resulted in low electrical contact resistance [16]. These samples exhibited a very low value of R_s ($0.73 \Omega \cdot \square^{-1}$) and a high value of T (93%). The Ni-NF demonstrated excellent performance characteristics, including reversible bendability for over 2000 cycles, high stretchability of up to 300%, an extremely low sheet resistance of $R_s = \sim 0.73 \Omega \cdot \square^{-1}$, and the ability to achieve heating temperatures of up to $280 \text{ }^\circ\text{C}$ at 1.5 V when employed as resistive heaters.

Jo *et al.* [19] reported a hybrid heater (Fig. 7a) for Cu and Ag NW prepared *via* electrospinning/electroplating and supersonic spraying, respectively. The resultant hybrid structures yielded values of $R_s = 0.18 \Omega \cdot \square^{-1}$ and $T = 91\%$. The hybrid film exhibited multifunctional features for heating and thermal-sensing applications. The uniformly distributed AgNWs acted as a bridge between the Cu fibers and provided a channel for efficient thermal transport. Thus, at an applied bias of 1.2 V, a hybrid heater can increase the temperature up to $60 \text{ }^\circ\text{C}$.

Lee *et al.* [123] reported a junction-free Ag nanonetwork (AgNN) based on the thermal deposition of PVP fibers on PET coated with fluorinated organic compounds (poly (heptadeca fluorodecyl methacrylate) (PFDMA):trichloro (perfluorooctyl) silane (FTS)) that act as a metal-repelling layer delivering junction-free contacts over a large area of $8 \text{ cm} \times 8 \text{ cm}$ (Fig. 7b). FTS exhibited a zero-condensation coefficient for Ag vapor. Note that 3-mercaptopropyl trimethoxysilane (MPTMS) and 3-aminopropyl trimethoxysilane (APTMS) with PVP were used for electrospinning, where the siloxane linkages of APTMS improved the mechanical strength of PVP, and the thiol moiety of MPTMS improved Ag binding. The SEM images depict the cross section of the AgNN. The fibers are flexible and exhibit heating characteristics, as shown in the IR image. This thin AgNN achieved a temperature of $180 \text{ }^\circ\text{C}$ at 5 V in 50 s.

Alloy-based coatings, such as Cu/Ni or Ni/Ag, and metal glasses (MG), such as Cu/Zr, can exhibit low sheet resistances; therefore, they are gaining attention for TMF applications [2,20]. An *et al.* [124] reported co-sputtered Cu/Zr on sacrificial polymer fibers and transferred it

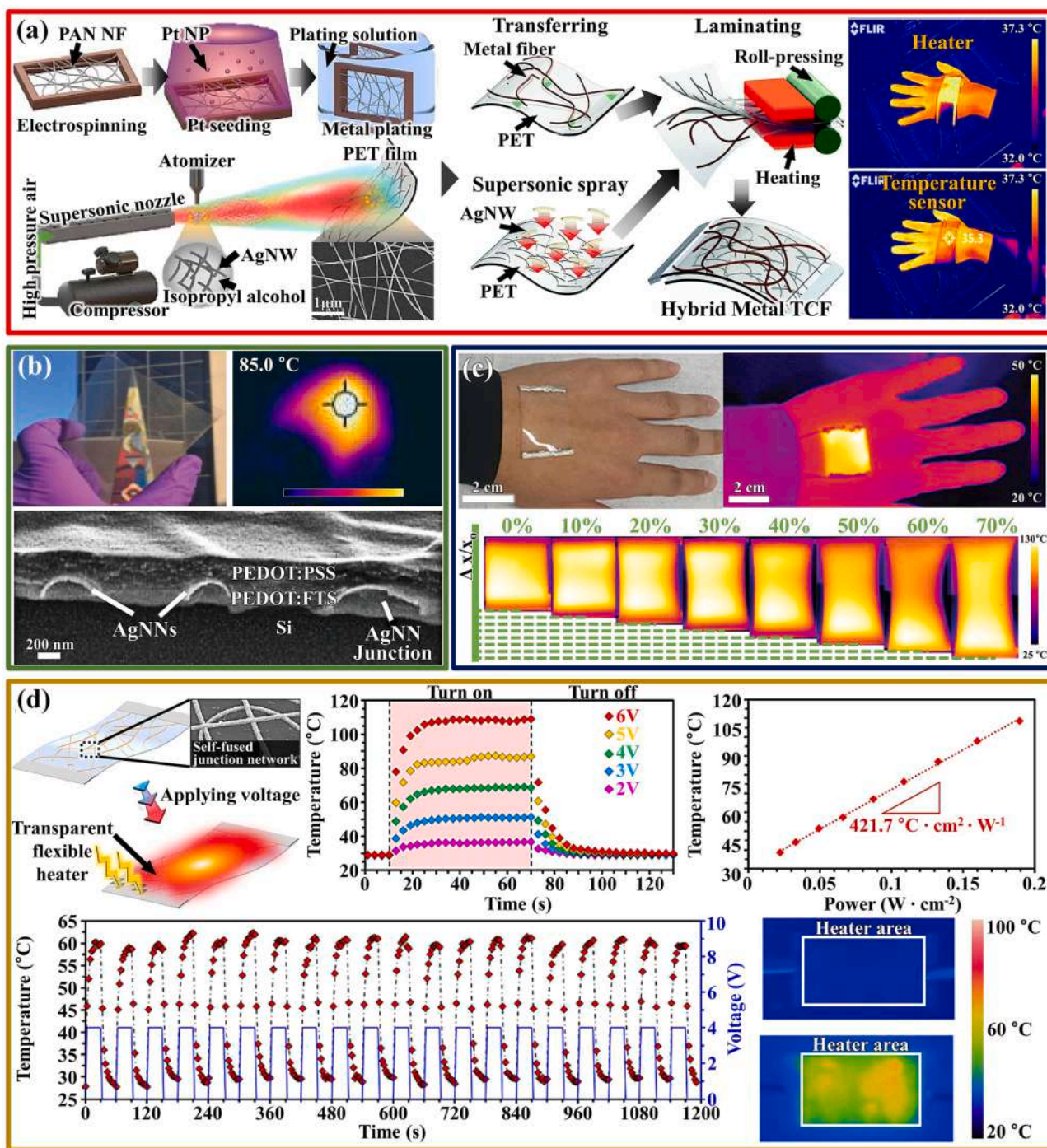


Fig. 7. (a) Schematic of TMF and supersonically sprayed AgNW electrodes and snapshots demonstrating wearable transparent sensor and heater. Reprinted from [19] 2018 © permission conveyed through Copyright Clearance Center, Inc. (b) Snapshot displaying PEDOT:PSS coated Ag network, IR image, and SEM image. Reprinted from [123] ©2020, Wiley-VCH GmbH. (c) Stretchable CuZr heater and IR images under stretching conditions [124] ©2016, American Chemical Society. (d) Cu/Ni-based heater, temperature, power, and transient profiles. IR images of heater at 0 and 4 V [2] ©2018, American Chemical Society.

to PDMS. These fibers exhibited mechanical robustness when the resistance change was less than 30%, even after being strained by 70% *via* stretching. In addition to stretchability, the heaters were transparent and body-attachable (Fig. 7c). The heaters at an applied bias of 7 V exhibited an increase in the temperature up to 180 °C.

Yoshikawa *et al.* [2] demonstrated a junction-less Cu/Ni NN prepared on poly (vinyl butyral) (PVB) fibers *via* electroless deposition. The performance of the heater was monitored by applying a DC voltage. The temperature increased with the applied voltage and reached the maximum level at 15 s in each case (Fig. 7d). In heaters, when a constant

DC voltage (V_a) is applied to the TMF, heat is generated by the Joule effect owing to the power (P) supplied to the heater, according to the following equation [21]

$$P = V_a^2 / R, \quad (2)$$

where R denotes the total resistance. The heat (H) released by the heater over time (t) is given by $H = IV_a t$, indicating that to achieve high current (I) or power, the resistance should be low. Moreover, the generated heat is the sum of conduction, convection, and radiation losses. When the

temperature is below 300 °C, the conductive heat loss become negligible. Thus, Q_{loss} can be expressed as follows [2,110]:

$$Q_{\text{loss}} = hA(T_s - T_a), \quad (3)$$

where h denotes the convective heat-transfer coefficient, A denotes the surface area of the heater, T_s denotes the steady-state temperature, and T_a denotes the ambient temperature. Thus, the heat transfer coefficient should be higher when the power was higher, indicating that the resistance should be low. Power efficiency is a crucial issue in the utilization of TMF in heaters. The power efficiency reported by Yoshikawa *et al.* [2] in Fig. 7d is determined from the slope of the surface temperature as a function of power consumption per unit area. The transient curves of heating and cooling by switching the voltage between 0 and 4 V depicts an increase in the temperature up to 60 °C. The increase in temperature was confirmed by IR images. The rapid rise in temperature confirms the suitability of the heater for defrosting/deicing applications. Such prominent heating is attributable to the lower thermal loss caused by the presence of junction-less metallic fibers. Further, highly transparent heaters have higher resistance; thus, to realize high-power Joule heating, higher applied voltages are needed [2,110]. Table 3 lists various metals and their respective applied voltages and temperature details [11,126]. The highest temperature can be achieved using Ag-based fibers, and maximum power can be used if the sheet resistance is low.

3.3. Transparent metallic fiber electrodes for solar cells

TCEs are indispensable for solar cell fabrication. Commercial ITO is used as a TCE; however, it increases the cost of fabrication owing to the use of a rare element of indium. Additionally, ITO is brittle, resulting in cracking during the application of a torsion force; this limits its application in wearable optoelectronics [23,71]. Moreover, the specular transmittance of ITO having a sheet resistance of $25 \Omega \cdot \square^{-1}$ is less than 80% for a wavelength of up to 600 nm. To address these issues, several studies on metallic fibers have been evaluated to determine the feasibility of such alternatives in flexible or superior solar cells.

The millimeter-wide finger-patterned busbar of metal on the front side of commercial crystalline silicon solar modules and flexible copper indium gallium selenide (CIGS) cells provides high electrical conductance for efficient electron transport. However, these wide grid patterns block the absorption of incident light and reduce device efficiency [44]. The reports of TMF with high transparency (90%) and low sheet resistance ($0.18 \Omega \cdot \square^{-1}$) have demonstrated promising potential for use on the front side of the solar cell as a TCE. The TMF can be prepared by two approaches: top-to-bottom (fiber deposition onto metal, metal etching,

and, finally, polymer removal (Fig. 8a) [122,127] or bottom-to-top (fiber deposition and metallization using various processes, such as electrodeposition and electroless coating) [41,44]. Wu *et al.* [12] suggested that copper fibers with an average fiber diameter of 50–200 nm are excellent TMFs owing to their high aspect ratio ($\sim 100,000$) and very low percolation critical density of $\sim 5.7 \times 10^{-8} \mu\text{m}^{-2}$ compared to that of CNT or Ag. Moreover, the fused junction yielded a much lower junction resistance than the CNT junction resistance or the boundary resistance of graphene [12]. Fig. 8a shows a straightforward approach for the fabrication of TMFs used in organic solar cells. The snapshots show the excellent conductivity and transparency of the TMFs [127]. The SEM image indicates a long continuous fiber, which is essential for achieving a high aspect ratio. Additionally, Wu *et al.* [12] demonstrated the excellent flexibility of TMFs deposited on PDMS using SEM images. Moreover, they sputtered metal (copper) on PDMS and bent the film under the same conditions, resulting in a large crack in the sample.

Cho *et al.* [44] suggested that metal nanofiber networks obtained using two different approaches could be a viable alternative for achieving a high cross-sectional aspect ratio compared to wide metal grids. These metal nanofiber networks exhibit high scattering, which is beneficial for exciting electrons in solar cells. Additionally, such a TMF exhibits high diffusive transmittance that can substitute for specular transmittance, owing to an effective increase in the path length of light absorption in the active layer, and subsequently enhance the solar cell performance [44]. Ni microfibers (NiMFs) prepared as alternatives to conventional metal grids were applied to CIGS solar cells. The SEM image (Fig. 8b) reveals the electroplating time, which mainly influences the TMF diameter [44].

The transmittance of NiMFs at a 550-nm (T_{550}) wavelength with electroplating times of 20 s, 25 s, and 30 s was 97.5%, 94.8%, and 93.1%, respectively (Fig. 8b), indicating that the shorter the electroplating time, the higher will be the transmittance. R_{sh} of these NiMFs was 2.35, 1.61, and $0.91 \Omega \cdot \square^{-1}$, respectively. These significantly low R_{sh} values were attributed to the large volume and high cross-sectional aspect ratio (height-to-width) of the NiMFs. Conversely, when the polyvinyl-alcohol (PVA)-based fiber was coated with platinum via sputtering for 3 min, it produced a high R_{sh} value of $275 \Omega \cdot \square^{-1}$ and $T_{550} = 94\%$, which could be due to a thin and incomplete Pt coating [71]. The sputtering process can coat the fibers on the line-of-sight surfaces, and the area under the shadow region remains uncoated compared with those of other transparent conductive materials of other dimensions, such as thin films and nanostructures. In both reports [44,71], transmittance was almost flat in the UV-to-visible wavelength region, unlike the ITO films, which exhibited peak transmittance near 550 nm.

The patterned grids of 100- μm -wide busbars and 25- μm -wide finger

Table 3
TMF for heater application.

Metal	Polymer fiber	R_s [$\Omega \cdot \square^{-1}$]	T [%]	Applied voltage [V]	Temp. [°C]	Substrate	Metal coating technique	Ref
ITO	–	50	83	4.5	29	PET	–	[125]
Ag NW	–	10	83	4.5	54	PET	–	
Ag NF	–	0.5	83	4.5	249.5	PET	Ink	
Ni/Ag microfiber	PAN	0.18	92	1.6	209	No substrate	Electroplating	[20]
Ag/ C mesh	PAN	2.7	91	3	280	PET	Electroplating	[64]
Cu/Ag NW	PAN	0.18	88	1.2	60	PET	Electroplating/cold spray	[18]
Ag	PVA	1.49	86.7	4	80	Norland optical adhesive	Thermal deposition	[110]
Ag	PVP	6.3	90	7.8	180	PET	Thermal deposition	[123]
Ag/rGO	PVB	3.3	91	7	360	PDMS	Electroless plating	[11]
Ni fiber	PAN	0.73	93	1.5	280	No substrate	Electroplating	[18]
Cu fiber	PAN	0.058	90	5.5	328	Glass	Electroplating	[110]
Cu	PVP	1	78	7	90	Flexible substrate	Electroless plating	[21]
Cu nanofiber	PVP	4.9	90	9	140	Glass	Electroplating	[75]
Cu microfiber	PVAc	2.58	88.7	3	180	PI film	sputtering	[126]
Cu/Ru	PVP	10	88	3	180	PET	Electroless plating	[80]
Cu/Ni	PVB	14	71	6	109	PET	Electroless plating	[2]
Cu/Zr	PVP	3.8	90	7	180	PDMS	Co-sputtering	[124]

PVB – polyvinylbutyral, PVAc – polyvinylacetate.

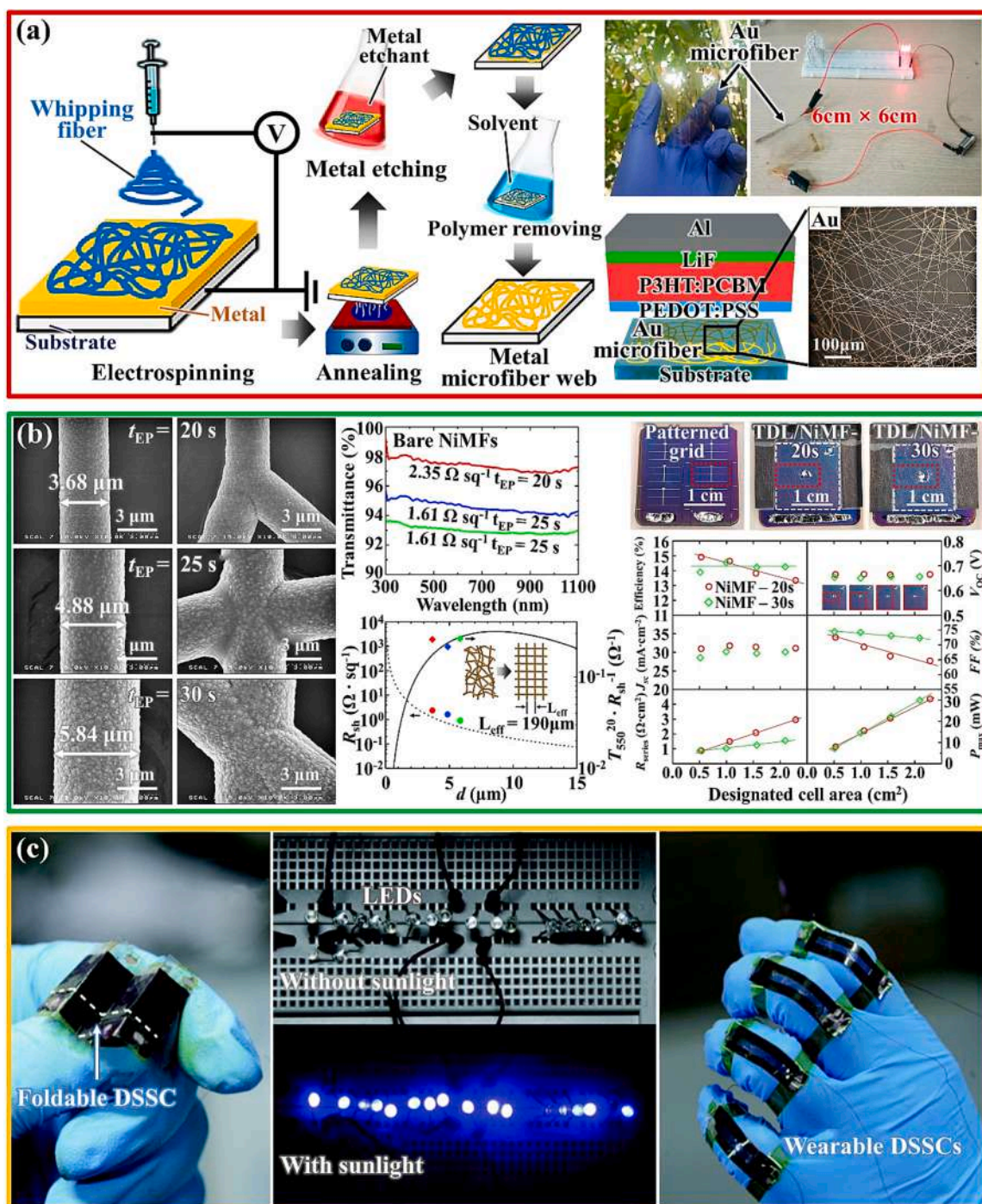


Fig. 8. (a) Schematic depicting Au-TMFs fabrication and its snapshots and SEM image [127] ©2015, American Chemical Society. (b) SEM images, transmission spectra, and sheet resistance of NiMFs prepared at different electroplating times. Fabricated solar cell devices with patterned grid, TDL/NiMF-20s, and TDL/NiMF-30s with the photovoltaic performance. Reprinted from [44] ©2019 Elsevier. (c) Foldable DSSC using Pt-nanotrough and TiO_2 . Reprinted from [71] 2015 © permission conveyed through Copyright Clearance Center, Inc.

patterns were visible to the naked eye (Fig. 8b). Conversely, the NiMFs deposited for 20 and 30 s were not visible and were covered with a transparent diffusive layer (TDL). By applying TDL/NiMF-20 s instead of the patterned grid, the short circuit current density (J_{sc}) was improved to $\sim 1.76 \text{ mA cm}^{-2}$. The enhanced J_{sc} was attributed to the substantial enhancement of diffusive transmission, resulting from the presence of the TDL. The TDL extends the optical path length in CIGS, ultimately improving the photogeneration of charges.

The area-dependent solar cell efficiency with NiMFs deposited for 20 and 30 s was examined by selecting cell areas of ~ 2.25 , 1.5, 1.0, and 0.5

cm^2 (inset of Fig. 8b) obtained *via* mechanical scribing. The solar cell efficiency ($\sim 14.2\%$) of the NiMF-30 s sample exhibited negligible difference with an increase in the cell area, whereas that of the NiMF-20 s sample decreased from 14.9% to 13.3%. The efficiency declined with a decrease in the fill factor (FF) in the area, owing to an increase in the series resistance (R_{series}). The FF improved for larger solar cell areas in the NiMF-30 s case owing to the thicker NiMF caused by its low resistance, whereas the thinner NiMF improved the transmittance and, in turn, J_{sc} . This indicates that highly transparent conductive NiMFs can be a good substitute for patterned film grids in the fabrication of efficient

and aesthetically superior solar cells and modules.

Wu *et al.* [12] applied Cu nanofiber networks to a transparent anode of the poly(3-hexylthiophene):phenyl-C61-butyric acid methyl ester (P3HT:PCBM) solar cell. The power conversion efficiency of the device with the Cu nanofiber network was 3.0%, and with regard to the solar cell properties, the values of J_{sc} , open circuit voltage (V_{oc}), and FF were $10.4 \text{ mA}\cdot\text{cm}^{-2}$, 0.55 V, and 0.53, respectively, which were comparable to those of glass/ITO devices ($J_{sc} = 10.3 \text{ mA}\cdot\text{cm}^{-2}$, $V_{oc} = 0.53 \text{ V}$, and FF = 0.66).

Kim *et al.* [128] used Pt nanofiber networks as transparent counter electrodes in DSSCs. They fabricated DSSCs using N719 dye-adsorbed TiO_2 films and Pt nanofiber networks with a liquid electrolyte. They used Pt nanofiber networks with resistances of 71 (Ω) (electrospinning time = 12 min) and $135 \Omega\cdot\text{cm}^{-1}$ (electrospinning time = 9 min). Although V_{oc} and J_{sc} were the same (0.81 V and $12.3 \text{ mA}\cdot\text{cm}^{-2}$), with a decrease in R_s , the overall photoelectric conversion efficiencies (η) increased to 5.3% and 6.0% owing to the increase in FF to 53.8% and 60.4%. They reported that the network structure of the Pt nanofibers was responsible for high electrochemical catalytic activity and high conductivity for electron transport. Similarly, Zhou *et al.* [71] reported TiO_2 -nanoarray-based flexible DSSCs using a Pt nanotrrough as the TCE (Fig. 8c). The cell exhibited a photoconversion efficiency of 3.82%, and >90% retention was observed after 200 bending cycles. The metal nanotrroughs were fabricated using PVA nanofibers, followed by Pt sputtering and PVP removal by water dissolution. Thus, the excellent transparency and conductivity of TMFs improve the efficiency and FF of solar cells, suggesting that TMFs are an alternative to brittle TCE (ITO-based substrates).

3.4. TMF as current collectors for transparent supercapacitors

Energy storage devices are power sources for modern devices and technologies. Transparent and flexible supercapacitors have recently

attracted attention for powering skin-attachable devices while satisfying aesthetic requirements [129,130]. To realize a transparent supercapacitor with high performance, the material must be substrate-free or deposited on a transparent substrate (e.g., ITO/PET). In addition to the superior electrochemical properties of the electrodes, such as high capacitance and stable performance over a wide operating voltage window, they must exhibit electro-optical transmittance and mechanical durability during bending and stretching [5,131].

Singh *et al.* [131] reported AgNF/PEDOT:PSS as a supercapacitor aligned with Norland optical adhesive 63 (NOA63) using a peel-off process. The electrodes exhibited good bending characteristics with a sheet resistance and transmittance of $2.12 \Omega\cdot\text{cm}^{-1}$ and 84.7%, respectively. AgNF (250–300-nm-thick Ag) serves the dual purpose of providing transparency and conducting pathways for current collection in the described system. PEDOT:PSS is well known for its charge storage characteristics and transparency. The resulting hybrid transparent supercapacitor electrode demonstrates an areal capacitance of $3.64 \text{ mF}\cdot\text{cm}^{-2}$ with 85% transmittance [131]. The same group reported the core-shell structure of a MnO_2 @Au nanofiber network for transparent supercapacitor electrodes [131]. Metal oxides suitable for supercapacitors are opaque. However, the selective electrodeposition of MnO_2 and the thermal deposition of Au on electrospun PVA nanofibers act as pseudocapacitors and current collectors, respectively. This core-shell structure (Fig. 9a) exhibited an outstanding balance between the capacitance ($8.26 \text{ mF}\cdot\text{cm}^{-2}$) and transmittance (86%) (Fig. 9b) of the supercapacitor electrode [131]. The flexible transparent symmetric supercapacitor assembled using MnO_2 @AuNF and PVA/LiCl as a gel electrolyte and separator (the inset shows a transparent symmetric supercapacitor attached to a marker) exhibited a transmittance of 79% and capacitance of $2.07 \text{ mF}\cdot\text{cm}^{-2}$. Moreover, the supercapacitor exhibited robust mechanical flexibility (Fig. 9c) at bending radii of 2–10 mm, with almost similar CV curves at $100 \text{ mV}\cdot\text{s}^{-1}$.

Lee *et al.* [5] reported transparent and stretchable MnO_2 /Au

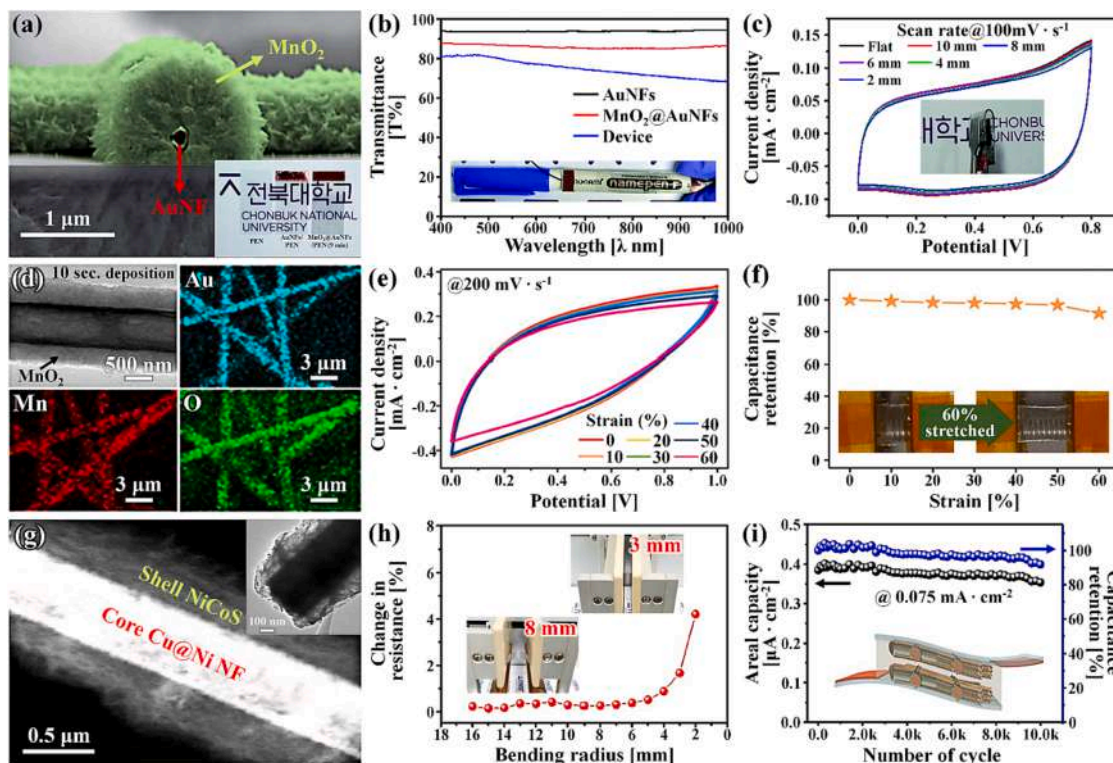


Fig. 9. Transparent and flexible electrodes for supercapacitor applications: (a) MnO_2 @AuNF morphology, (b) transmittance, and (c) cyclic voltammetry curves under bending. Reprinted from [129] 2019 © permission conveyed through Copyright Clearance Center, Inc. (d) TEM and elemental mapping of MnO_2 @AuNF. (e) Cyclic voltammetry curves. (f) Capacitance retention under strain. Reprinted from [5] ©2020 Elsevier. (g) Electrodeposited NiCoS nanosheets on Cu@Ni NF. (h) Impact of bending on resistance. (i) Long-term cycling performance. Reprinted from [70] ©2020 Elsevier.

nanofiber networks. Polymethyl methacrylate fibers were electrospun and coated with gold *via* ion sputtering. The fibers were then transferred to the PDMS. MnO₂ was then electrodeposited at a potential of 1.5 V. Electrodeposition allows the uniform and conformal deposition of MnO₂ on the Au NF. This is indicated by TEM and elemental mapping illustrated in Fig. 9d. The PDMS allows easy stretchability tests of MnO₂@AuNF. The fabricated supercapacitor device was highly stretchable, with a stretchability of 60%, transmittance of 54%, and areal capacitance of 3.68 mF·cm⁻². The capacitance retention was 96% after 8400 stretching cycles (Fig. 9e and 9f). No significant change in capacitance was observed in bending tests, whereas capacitance retention decreased to 95% and 88% at twisting angles of 90° and 120°, respectively.

Soram *et al.* [70] reported low-cost high-performance Cu–Ni metal network-based TEs for gold. The combination of Cu and Ni addresses the oxidation problem of Cu and improves the electrochemical stability at high pH. Further, battery-type NiCoS was grown *via* electrodeposition, forming a shell of NiCoS-intertwined nanosheets (Fig. 9g) over Cu (70 nm)–Ni (30 nm)–coated PVA NF. The optimized Ni(0.8):Co(0.2)-S catalyst exhibited a porous structure, rich electroactive redox sites,

and high transmittance. Subsequently, the NiCoS-coated Cu–Ni NF was transferred to the polyethylene naphthalate (PEN) substrates. The electromechanical bending properties of NiCoS@Cu–Ni on PEN (Fig. 9h) showed a negligible change in resistance at different bending radii of 4–16 mm. The solid-state symmetric supercapacitor exhibited a transmittance of 65% with an areal capacity of 1.51 μAh·cm⁻² at 10 mV·s⁻¹ (Fig. 9i). At a current density of 0.075 mA·cm⁻², it exhibited a capacity of 0.37 μAh·cm⁻² with a capacity retention of 92% after 10,000 cycles. Notably, NiCoS is a battery-type material; therefore, the areal capacity is reported instead of the areal capacitance.

Evidently, TMFs have been successfully used in supercapacitors. As a current collector, the overall transparency of the device critically depends on the transparency of the materials. Ag and Au are stable, whereas the stability of Cu can be improved by coating it with Ni. Au has been widely used as a current collector owing to its high electrical conductivity, availability, ease of processing, and electrochemical stability. Au coated with MnO₂ exhibited a transmittance of 79% and capacitance of 2.07 mF·cm⁻² for a symmetric supercapacitor, which is the highest among reported values. Furthermore, flexible electrochromic energy storage devices are in demand for use in wearable

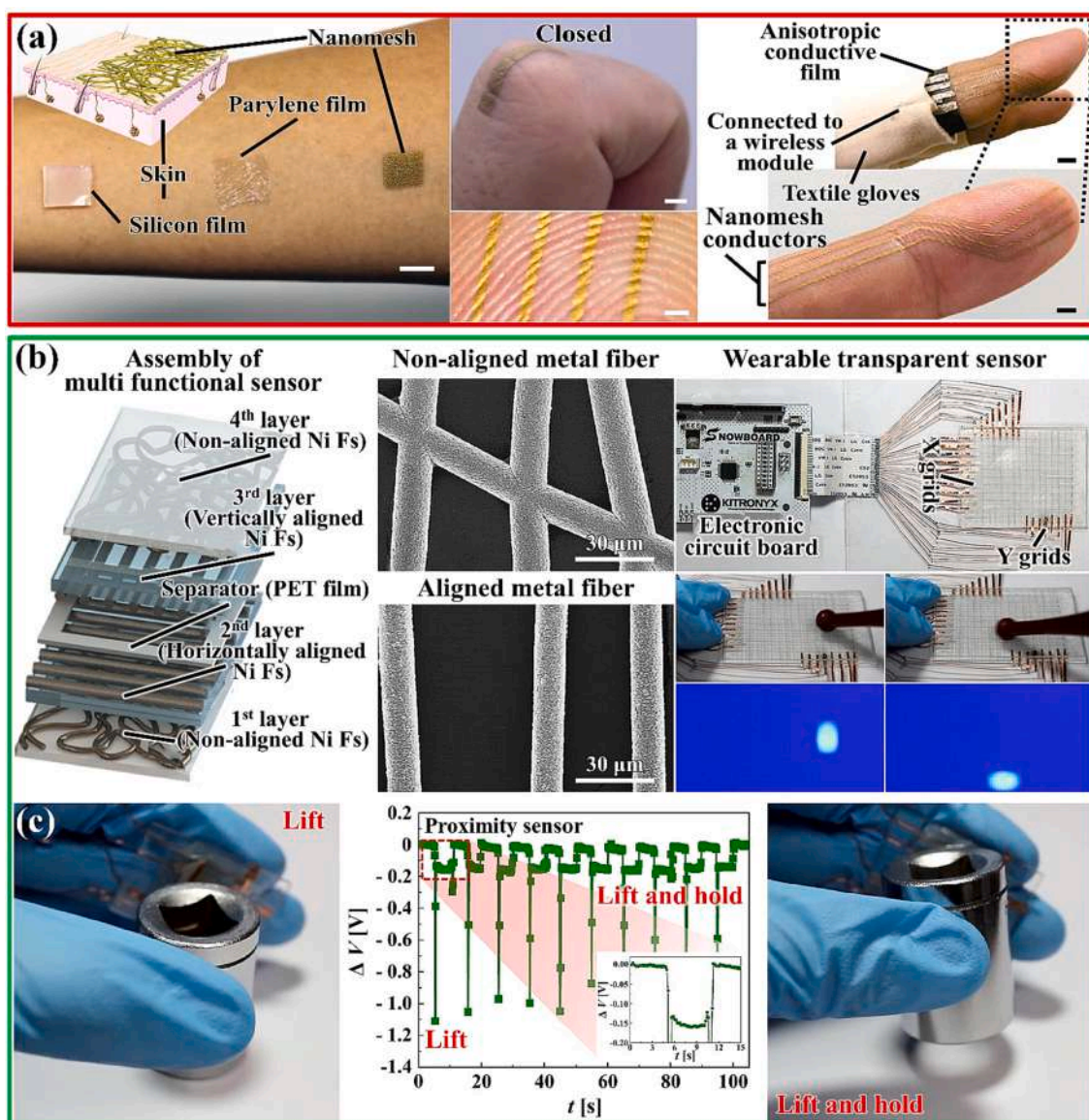


Fig. 10. Proof of concept of a wearable multifunctional sensor: (a) Laminated human skin [133] ©2017, Springer Nature, (b) assembly of multifunctional sensor using aligned and non-aligned TMF as a pressure sensor and (c) finger-tip patch for proximity sensor [52] ©2020 Springer Nature.

devices and smart windows [132]. Using an active electrochromic material changes device transparency, which is an indicative of the level of energy stored. It should be noted that TMFs have not been used in electrochromic supercapacitors.

3.5. Wearable and e-skin electronics

Electronic skin (e-skin) or artificial skin that replicates the sensing ability of a real skin is necessary to develop multisensory surfaces for artificial intelligence (robots) and medical diagnostics. Health monitoring sensors are an integral part of HMIs in modern wearable electronics for adopting healthier lifestyles. Advancements in technology have expedited real-time monitoring of various parameters using wearable electronics, such as pressure sensors [74,134]. Moreover, transparent health monitoring devices for real-time diagnosis are beneficial for obtaining visual information. Recently, Won *et al.* [10] suggested that transparent e-skin sensors for optogenetics are beneficial because they do not block light or hinder the activity of cells, such as neurons. Therefore, multifunctional e-skin has gained attention owing to its ability to collect information beyond the sensory function layers of the skin [3,135].

Real-time monitoring using inflammation-free and soft-material-based e-skin sensors has been investigated owing to its non-invasiveness and comfort [3,136,137]. Miyamoto *et al.* [133] prepared metalized electrospun fiber-based e-skin sensors and laminated them on human skin (Fig. 10a) for use as temperature and pressure sensors. Recently, Peng *et al.* [138] developed a self-powered real-time respiratory monitoring sensor to diagnose apnea and hypopnea, which are related to obstructive sleep. Metalized electrospun fiber-based sensors are three-dimensional hierarchical structures with macro-to-nanopores that are highly sensitive and require minimal-to-no power for their operation.

E-skin sensors are permeable and require high conductivity. Considering the need for superior conductivity, Ma *et al.* [139] reported an electrocardiogram and sweat stretchable sensor using eutectic gallium–indium alloy with biocompatible polystyrene-butadiene-butylbenzene-butylbenzene exhibiting a conductivity of $10,000\text{--}1,800,000\text{ S m}^{-1}$, corresponding to their weight of $0.8\text{--}5\text{ mg}\cdot\text{m}^{-2}$. However, reports consistently suggest that a trade-off exists between conductivity and quality factors. E-skin electronics now reach the HMI level, where the pressure sensor reads the body motions and transfers the signal, which can be mimicked by robots. The use of HMI sensors has recently been demonstrated by Dong *et al.* [140]. The sensors were prepared using electrospun skin-electronics-based stretchable (SEBS) nonwoven microfibers that were stencil-printed with liquid metal. The use of liquid metal is cost-effective as it can be recycled by centrifugation (Wang *et al.* [141]). Wang *et al.* [55] reported the use of AgNF in skin mountable hyperthermia patches (HTPs) that provide uniform heating at low voltage for tumor treatment. High optical transparency allows real-time inspection of subcutaneous tumors and prevents overheating and skin burns. HTPs are also effective in facilitating medical diagnostics, such as pulse oximetry. Seo *et al.* [56] reported an Au nano-network (Au NN) microelectrode array-based electrocorticogram (ECoG) for implantable neural electronics. The flexibility of the ECoG provides conformal contact, and the Au NN provides a low photoelectric artifact owing to a low sheet resistance of $7\text{ }\Omega\cdot\text{cm}^{-1}$. Such an ECoG provides efficient visualization of neural activities and allows an accurate interpretation of neural dynamics, thus rendering Au NN significant for biomedical applications. Similarly, Au-coated flexible fibers were integrated with PEDOT:PSS and a hydrogel to create a smart commercial ocular contact lens [142]. The seamless integration of TMFs and hydrogel ocular contact lenses is promising for the diagnosis of glaucoma and diabetes. Moreover, the use of these devices in the medical field with augmented reality reduces the complexity involved in the diagnosis of internal diseases and surgeries. These reports provide insight into the possible upgrade of health-monitoring

systems and artificial intelligence in the era of the IoT.

The multifunctionality of sensors or e-skin are desirable for efficient health monitoring system with cost-effective devices. For such multifunctional sensors (proximity, thermal, or pressure sensor), the aligned or non-aligned electrospun fibers plays a significant role. In this regard, the multifunctional sensor assembly reported by Jo *et al.* [52] used Ni-electroplated nonaligned and aligned PAN nanofibers separated by a PET film (Fig. 10b). A wearable soft-material proximity sensor was subjected to 10 test cycles. The proximity sensor exhibited a response time as indicated by a sudden voltage drop (0 to -1.1 V) upon bringing the sensor close to an object. The proximity sensor displayed excellent sensitivity, as lifting the object caused the voltage to rapidly approach -0.15 V and remain constant until the object was released. Jo *et al.* [52] revealed that it is important to optimize the electrospinning and electroplating times of the metallized fibers to obtain low sheet resistance (aligned: $1.99\text{ }\Omega\cdot\text{cm}^{-1}$; nonaligned: $0.14\text{ }\Omega\cdot\text{cm}^{-1}$), which is necessary for the swift response time of the sensors. The excellent sensitivity and multifunctionality of these TMFs is promising for development of next-generation anthropomorphic robots.

Fig. 11 summarizes the various applications of TMFs. TMFs with high transparencies, low sheet resistances, flexibilities, and stretchability are potential alternatives to ITO. The development of multifunctional sensors with TMFs combined with artificial e-skin or proximity sensors can lead to a considerable revolution in the health sector [44,52,143].

4. Outlook and conclusions

Transparent metallic fiber use has grown exponentially in various applications, such as touchscreens, solar cells, supercapacitors, heaters, and e-skin. However, the simultaneous attainment of low sheet resistance and high transmittance of TMF is challenging, and their integration into commercial wearable electronics requires increased attention. Fabrication and material property innovations are critical for overcoming these challenges.

4.1. Fabrication techniques

One challenge in the fabrication of TMFs is the merging of nonaligned electrospun fibers that causes a significant increase in junction resistance and impacts transmittance. By contrast, aligned fibers reduce junction resistance but require customized electrospinning setups. Additionally, the reproducibility of aligned and nonaligned fibers depends significantly on the surrounding temperature and humidity, which vary widely with geographic location and the time of year. Thus, to enable widespread reproducibility of fibers, the ambient parameters must be reported and controlled. An additional challenge for uniform coatings is that electrospinning time and fiber diameter play vital roles in the metallization and control of the metal coating thickness. In this regard, electroless plating for metallization of fibers is reportedly a more appealing technique for conformal and thin coatings. By contrast, electroplating can yield a thick metal coating over the fibers, whereas physical vapor deposition techniques can yield thin metal coatings but sometimes lack full coverage of fibers owing to the shadowing effect. Nevertheless, this review suggests that the current state of these technologies is sufficient to produce highly conductive and transparent metal fibers.

4.2. Properties

The foremost advantageous property of electrospun TMFs is in their high volume-to-aspect ratio, which guarantees a relatively easy integration into flexible electronics. Furthermore, TMFs exhibit low junction resistance and offer a trade-off between sheet resistance and transmittance that depends on the metal selection and the technique for coating of electrospun fibers. The flexibility of TMFs and TMF-based wearable electronics is essential for health monitoring and sports-



Fig. 11. Applications of TMFs as transparent conducting electrodes: (a) Photovoltaic devices [44] (©2019, Elsevier), (b) touchscreen panels [143] (©2014, American Chemical Society) (c) heaters, (d) e-skin, (e-g) thermal, proximity and pressure sensors for health monitoring [52] (© 2020, Springer Nature).

training applications and the demonstration of 100,000 bending cycles without a significant change in performance affirms the superior flexibility of the TMFs. Furthermore, stretchability is essential for providing stability during mechanical deformation that occurs when wearing smart apparel [13]. However, flexible electronics must be stretchable when woven into fabric and research on stretchable TMFs for next-generation wearable electronics remains at the early stages of development.

4.3. Integration

Stretchability is also required for the integration of various components, such as LEDs, photodetectors, and photovoltaics (PVs), for body/shape-adaptable wearable electronics. However, fabricating these components simultaneously on a single stretchable platform is complex and tedious owing to their pattern requirements with small feature sizes. Electrospinning is a versatile technique for fabricating flexible fibers that become mechanically strong and highly conductive upon metallization; consequently, TMFs fabricated with electrospinning are emerging as a superior alternative to brittle and expensive ITO. This review discusses multifunctional TMFs for various applications (including in touchscreens, transparent heaters, solar cells, transparent supercapacitors, LEDs, and sensors). These TMFs exhibit low sheet resistance and optimal transmittance, thus rendering them suitable for use in prominent applications, including e-skins and wearable electronics. Significant improvement in the figure of merit, from $2.8 \times 10^{-3} \Omega^{-1}$ (Pt-TMFs) to $652 \times 10^{-3} \Omega^{-1}$ (Ag-Cu core-shell fibers), has been achieved in recent years. Interestingly, each metal coating technique has unique features. For instance, PVD provides excellent surface smoothness, electroless plating is well-known for conformal coating, and electroplating is suitable for developing customized nanostructures, such as nanocones and thorns. Notably, the formation of customized nanostructures via electroplating is highly dependent on the metal sources and electrodeposition conditions.

The stretchability of wearable electronics such as touchscreen sensors can be improved using a hierarchical mesh (web-in-web structure) and multiorientation arrangements of TMFs. The transmittance characteristics of TMFs are not required for touchscreens; however, TMFs must be highly transparent (>90%) for solar cells and LEDs. Thus far, TMFs fabricated using Au have been found to be the most flexible, exhibiting stable performance even after 100,000 bending cycles, owing

to their superior ductility. Ni-based TMFs are used in solar cells as replacements for metal grids to enhance solar cell efficiency and current density. Pt-based TMFs are often used in dye-sensitized solar cells (DSSCs) because of their excellent electrochemical stability. The multifunctionality of patch sensors allows them to send signals to health monitoring devices for real-time diagnosis. In addition, patch sensors such as ECoG are used to monitor and treat neurological disorders such as epilepsy. Various wearable electronics, such as touchscreens and e-skins, are devices with low power consumption and flexible and transparent supercapacitors are suitable for powering these devices because of their long life and ease of integration. In summary, TMFs provide features such as flexibility and stretchability that accelerate development of HMIs and, consequently, indium-free TMFs are rapidly replacing conventional brittle ITO-based TCEs in wearable electronics.

Declaration of Competing Interest

The authors declare that they have no known competing financial interests or personal relationships that could have appeared to influence the work reported in this paper.

Data availability

No data was used for the research described in the article.

Acknowledgments

This work was supported by the National Research Foundation of Korea (NRF) grant funded by the Korea government (MSIT) NRF-2020R1A5A1018153.

References

- [1] J. Wang, W. Yang, Z. Liu, Y. Su, K. Li, Y. Li, Q. Zhang, C. Hou, H. Wang, Ultra-fine self-powered interactive fiber electronics for smart clothing, *Nano Energy* (2023), 108171.
- [2] R. Yoshikawa, M. Tenjimbayashi, T. Matsubayashi, K. Manabe, L. Magagnin, Y. Monnai, S. Shiratori, Designing a flexible and transparent ultrarapid electrothermogenic film based on thermal loss suppression effect: A self-fused Cu/Ni composite junctionless nanonetwork for effective deicing heater, *ACS Appl. Nano Mater.* 1 (2018) 860–868.
- [3] H.S. Jo, C.-W. Park, S. An, A. Aldalbahi, M. El-Newehy, S.S. Park, A.L. Yarin, S. Yoon, Wearable multifunctional soft sensor and contactless 3D scanner using

- supersonically sprayed silver nanowires, carbon nanotubes, zinc oxide, and PEDOT:PSS, *NPG Asia Mater.* 14 (2022) 23.
- [4] V.H. Nguyen, D.T. Papanastasiou, J. Resende, L. Bardet, T. Sannicolo, C. Jiménez, D. Muñoz-Rojas, N.D. Nguyen, D. Bellet, Advances in flexible metallic transparent electrodes, *Small* 18 (2022), 2106006.
- [5] Y. Lee, S. Chae, H. Park, J. Kim, S.-H. Jeong, Stretchable and transparent supercapacitors based on extremely long MnO₂/Au nanofiber networks, *Chem. Eng. J.* 382 (2020), 122798.
- [6] Y. Zhao, H. Liu, Y. Yan, T. Chen, H. Yu, L.O. Ejeta, G. Zhang, H. Duan, Flexible transparent electrochemical energy conversion and storage: from electrode structures to integrated applications, *Energy Environ. Mater.* 6 (2023), e12303.
- [7] S. An, B. Joshi, A.L. Yarin, M.T. Swihart, S.S. Yoon, Supersonic cold spraying for energy and environmental applications: one-step scalable coating technology for advanced micro- and nanotextured materials, *Adv. Mater.* 32 (2020), 1905028.
- [8] J.C. Yeo, C.T. Lim, R.-K.-Y. Tong, Wearable sensors for upper limb monitoring, *Wearable Technol. Med. Health Care* 2018 (2018) 113–134.
- [9] M. Zhu, J. Zhang, W. Xu, R. Xiong, C. Huang, Cellulose-based fibrous materials for self-powered wearable pressure sensor: A mini review, *Cellul.* 30 (2023) 1981–1998.
- [10] D. Won, J. Bang, S.H. Choi, K.R. Pyun, S. Jeong, Y. Lee, S.H. Ko, Transparent electronics for wearable electronics application, *Chem. Rev.* (2023).
- [11] Y. Yang, S. Chen, W. Li, P. Li, J. Ma, B. Li, X. Zhao, Z. Ju, H. Chang, L. Xiao, Reduced graphene oxide conformally wrapped silver nanowire networks for flexible transparent heating and electromagnetic interference shielding, *ACS Nano* 14 (2020) 8754–8765.
- [12] H. Wu, L. Hu, M.W. Rowell, D. Kong, J.J. Cha, J.R. McDonough, J. Zhu, Y. Yang, M.D. McGehee, Y. Cui, Electrospun metal nanofiber webs as high-performance transparent electrode, *Nano Lett.* 10 (2010) 4242–4248.
- [13] T. Kim, C. Park, E.P. Samuel, S. An, A. Aldabahi, F. Alotaibi, A.L. Yarin, S. S. Yoon, Supersonically sprayed washable, wearable, stretchable, hydrophobic, and antibacterial rGO/AgNW fabric for multifunctional sensors and supercapacitors, *ACS Appl. Mater. Interfaces* 13 (2021) 10013–10025.
- [14] X. Wang, J. Plog, K.M. Lichade, A.L. Yarin, Y. Pan, Three-dimensional printing of highly conducting PEDOT: PSS-based polymers, *J. Manuf. Sci. Eng.* 145 (2022).
- [15] J. Plog, X. Wang, K.M. Lichade, Y. Pan, A.L. Yarin, Extremely-fast electrostatically-assisted direct ink writing of 2D, 2.5D and 3D functional traces of conducting polymer Poly(3,4-ethylenedioxythiophene) polystyrene sulfonate-polyethylene oxide (PEDOT:PSS-PEO), *J. Colloid Interface Sci.* 651 (2023) 1043–1053.
- [16] D. Wang, Y. Zhang, X. Lu, Z. Ma, C. Xie, Z. Zheng, Chemical formation of soft metal electrodes for flexible and wearable electronics, *Chem. Soc. Rev.* 47 (2018) 4611–4641.
- [17] K.-W. Seo, J. Lee, J. Jo, C. Cho, J.-Y. Lee, Highly Efficient (>10%) flexible organic solar cells on PEDOT-free and ITO-free transparent electrodes, *Adv. Mater.* 31 (2019), 1902447.
- [18] S. An, Y.I. Kim, H.S. Jo, M.-W. Kim, M.T. Swihart, A.L. Yarin, S.S. Yoon, Oxidation-resistant metallized nanofibers as transparent conducting films and heaters, *Acta Mater.* 143 (2018) 174–180.
- [19] H.S. Jo, H.-J. Kwon, T.-G. Kim, C.-W. Park, S. An, A.L. Yarin, S.S. Yoon, Wearable transparent thermal sensors and heaters based on metal-plated fibers and nanowires, *Nanoscale* 10 (2018) 19825–19834.
- [20] Y.I. Kim, S. An, M.-W. Kim, H.-S. Jo, T.-G. Kim, M.T. Swihart, A.L. Yarin, S. S. Yoon, Highly transparent, conducting, body-attachable metallized fibers as a flexible and stretchable film, *J. Alloy. Compd.* 790 (2019) 1127–1136.
- [21] H. Woo, S. Kim, S. Yoon, K. Kim, G.H. Kim, T. An, G. Lim, Highly flexible and transparent film heater with electrospun copper conductive network via junction-free structure, *J. Alloy. Compd.* 886 (2021), 161191.
- [22] Y. Wang, J.-T. Huang, Transparent, conductive and superhydrophobic cellulose films for flexible electrode application, *RSC Adv.* 11 (2021) 36607–36616.
- [23] H.-G. Im, B.W. An, J. Jin, J. Jang, Y.-G. Park, J.-U. Park, B.-S. Bae, A high-performance, flexible and robust metal nanotrough-embedded transparent conducting film for wearable touch screen panels, *Nanoscale* 8 (2016) 3916–3922.
- [24] J.T. Gudmundsson, A. Anders, A. von Keudell, Foundations of physical vapor deposition with plasma assistance, *Plasma Sources Sci. Technol.* 31 (2022), 083001.
- [25] D.T. Papanastasiou, A. Schultheiss, D. Muñoz-Rojas, C. Celle, A. Carella, J. P. Simonato, D. Bellet, Transparent heaters: A review, *Adv. Funct. Mater.* 30 (2020), 1910225.
- [26] R.J.B. Leote, M. Beregoi, I. Enculescu, V.C. Diculescu, Metallized electrospun polymeric fibers for electrochemical sensors and actuators, *Curr Opin. Electrochem.* (2022), 101024.
- [27] J. Yin, W. Ma, Z. Gao, X. Lei, C. Jia, A review of electromagnetic shielding fabric, wave-absorbing fabric and wave-transparent fabric, *Polymers* 14 (2022) 377.
- [28] K. Chatterjee, J. Tabor, T.K. Ghosh, Electrically conductive coatings for fiber-based e-textiles, *Fibers* 7 (2019) 51.
- [29] R. Hmshirazi, T. Mohammadi, A.A. Asadi, M.A. Tofighy, Electrospun nanofiber affinity membranes for water treatment applications: A review, *J. Water Process Eng.* 47 (2022), 102795.
- [30] C.V. Boys, On the production, properties, and some suggested uses of the finest threads, *Proc. Phys. Soc. Lond.* 9 (1887) 8.
- [31] F. Anton, Process and apparatus for preparing artificial threads, Google Patents (1934).
- [32] Y. Sun, X. Zhang, M. Zhang, M. Ge, J. Wang, Y. Tang, Y. Zhang, J. Mi, W. Cai, Y. Lai, Rational design of electrospun nanofibers for gas purification: Principles, opportunities, and challenges, *Chem. Eng. J.* (2022), 137099.
- [33] A.L. Yarin, B. Pourdeyimi, S. Ramakrishna, Fundamentals and applications of micro-and nanofibers, Cambridge University Press, 2014.
- [34] A.L. Yarin, Bending and buckling instabilities of free liquid jets: experiments and general quasi-one-dimensional model, in: N. Ashgriz (Ed.), Handbook of Atomization and Sprays: Theory and Applications, Springer, US, Boston, MA, 2011, pp. 55–73.
- [35] M. Lauricella, S. Succi, E. Zussman, D. Pisignano, A.L. Yarin, Models of polymer solutions in electrified jets and solution blowing, *Rev. Mod. Phys.* 92 (2020), 035004.
- [36] B. Joshi, E. Samuel, Y.-I. Kim, A.L. Yarin, M.T. Swihart, S.S. Yoon, Review of recent progress in electrospinning-derived freestanding and binder-free electrodes for supercapacitors, *Coord. Chem. Rev.* 460 (2022), 214466.
- [37] A. Greiner, J.H. Wendorff, Electrospinning: a fascinating method for the preparation of ultrathin fibers, *Angew. Chem. Int. Ed.* 46 (2007) 5670–5703.
- [38] Y. Wang, T. Yokota, T. Someya, Electrospun nanofiber-based soft electronics, *NPG Asia Mater.* 13 (2021) 22.
- [39] C. Turro, W.J. Dressick, Electroless Metallization of the elements: survey and progress, *ACS Appl. Electron. Mater.* (2022).
- [40] R. Yu, A. Senocrate, F. Bernasconi, T. Künniger, L. Müller, R. Pauer, C. Battaglia, X. Wang, J. Wang, Flexible and ultrathin waterproof conductive cellular membranes based on conformally gold-coated PVDF nanofibers and their potential as gas diffusion electrode, *Mater. Des.* 225 (2023), 111441.
- [41] X. Yang, X. Hu, Q. Wang, J. Xiong, H. Yang, X. Meng, L. Tan, L. Chen, Y. Chen, Large-scale stretchable semiembedded copper nanowire transparent conductive films by an electrospinning template, *ACS Appl. Mater. Interfaces* 9 (2017) 26468–26475.
- [42] M. Beregoi, C. Bustioci, A. Evangelidis, E. Matei, F. Iordache, M. Radu, A. Dinischioti, I. Enculescu, Electrochromic properties of polyaniline-coated fiber webs for tissue engineering applications, *Int. J. Pharm.* 510 (2016) 465–473.
- [43] M.-W. Kim, S. An, H. Seok, S.S. Yoon, A.L. Yarin, Electrostatic transparent air filter membranes composed of metallized microfibers for particulate removal, *ACS Appl. Mater. Interfaces* 11 (2019) 26323–26332.
- [44] D.-H. Cho, H.S. Jo, W.-J. Lee, T.-G. Kim, B. Shin, S.S. Yoon, Y.-D. Chung, Enhanced electrical conductivity of transparent electrode using metal microfiber networks for gridless thin-film solar cells, *Sol. Energy Mater. Sol. Cells* 200 (2019), 109998.
- [45] H. Park, H. Si, J. Gu, D. Lee, D. Park, Y.-I. Lee, K. Kim, Engineered kirigami design of PVDF-Pt core-shell nanofiber network for flexible transparent electrode, *Sci. Rep.* 13 (2023) 2582.
- [46] B. Joshi, E. Samuel, Y.-I. Kim, A.L. Yarin, M.T. Swihart, S.S. Yoon, Progress and potential of electrospinning-derived substrate-free and binder-free lithium-ion battery electrodes, *Chem. Eng. J.* 430 (2022), 132876.
- [47] D.H. Reneker, A.L. Yarin, H. Fong, S. Koombhongse, Bending instability of electrically charged liquid jets of polymer solutions in electrospinning, *J. Appl. Phys.* 87 (2000) 4531–4547.
- [48] M.W. Lee, S. An, S.S. Yoon, A.L. Yarin, Advances in self-healing materials based on vascular networks with mechanical self-repair characteristics, *Adv. Colloid Interface Sci.* 252 (2018) 21–37.
- [49] J. Xue, T. Wu, Y. Dai, Y. Xia, Electrospinning and electrospun nanofibers: Methods, materials, and applications, *Chem. Rev.* 119 (2019) 5298–5415.
- [50] S. Jana, A. Cooper, F. Ohuchi, M. Zhang, Uniaxially aligned nanofibrous cylinders by electrospinning, *ACS Appl. Mater. Interfaces* 4 (2012) 4817–4824.
- [51] M. Yousefzadeh, S. Ramakrishna, Modeling performance of electrospun nanofibers and nanofibrous assemblies, in: *Electrospun nanofibers*, Elsevier, 2017, pp. 303–337.
- [52] H. Seok Jo, S. An, H.-J. Kwon, A.L. Yarin, S.S. Yoon, Transparent body-attachable multifunctional pressure, thermal, and proximity sensor and heater, *Sci. Rep.* 10 (2020), 2701.
- [53] Y. Wang, J. Cheng, Y. Xing, M. Shahid, H. Nishijima, W. Pan, Stretchable platinum network-based transparent electrodes for highly sensitive wearable electronics, *Small* 13 (2017), 1604291.
- [54] Y.I. Kim, E. Samuel, B. Joshi, M.-W. Kim, T.G. Kim, M.T. Swihart, S.S. Yoon, Highly efficient electrodes for supercapacitors using silver-plated carbon nanofibers with enhanced mechanical flexibility and long-term stability, *Chem. Eng. J.* 353 (2018) 189–196.
- [55] Q. Wang, H. Sheng, Y. Lv, J. Liang, Y. Liu, N. Li, E. Xie, Q. Su, F. Ershad, W. Lan, A skin-mountable hyperthermia patch based on metal nanofiber network with high transparency and low resistivity toward subcutaneous tumor treatment, *Adv. Funct. Mater.* 32 (2022), 2111228.
- [56] J.W. Seo, K. Kim, K.W. Seo, M.K. Kim, S. Jeong, H. Kim, J.W. Ghim, J.H. Lee, N. Choi, J.Y. Lee, Artifact-free 2D mapping of neural activity in vivo through transparent gold nanonetwork array, *Adv. Funct. Mater.* 30 (2020), 2000896.
- [57] S. An, Y.I. Kim, S. Sinha-Ray, M.-W. Kim, H.S. Jo, M.T. Swihart, A.L. Yarin, S. S. Yoon, Facile processes for producing robust, transparent, conductive platinum nanofiber mats, *Nanoscale* 9 (2017) 6076–6084.
- [58] H. Wu, D. Kong, Z. Ruan, P.-C. Hsu, S. Wang, Z. Yu, T.J. Carney, L. Hu, S. Fan, Y. Cui, A transparent electrode based on a metal nanotrough network, *Nat. Nanotechnol.* 8 (2013) 421–425.
- [59] S. Sinha-Ray, Y. Zhang, A.L. Yarin, Thorny devil nanotextured fibers: the way to cooling rates on the order of 1 kW/cm², *Langmuir* 27 (2010) 215–226.
- [60] M.-W. Kim, S. An, H. Seok, A.L. Yarin, S.S. Yoon, Transparent metallized microfibers as recyclable electrostatic air filters with ionization, *ACS Appl. Mater. Interfaces* 12 (2020) 25266–25275.
- [61] K. Azuma, K. Sakajiri, H. Matsumoto, S. Kang, J. Watanabe, M. Tokita, Facile fabrication of transparent and conductive nanowire networks by wet chemical

- etching with an electrospun nanofiber mask template, *Mater. Lett.* 115 (2014) 187–189.
- [62] M. Adabi, M. Adabi, Electrodeposition of nickel on electrospun carbon nanofiber mat electrode for electrochemical sensing of glucose, *J. Dispers. Sci. Technol.* 42 (2021) 262–269.
- [63] G. Ercolano, F. Farina, S. Cavaliere, D.J. Jones, J. Rozière, Towards ultrathin Pt films on nanofibers by surface-limited electrodeposition for electrocatalytic applications, *J. Mater. Chem. A* 5 (2017) 3974–3980.
- [64] J.W. Huh, H.-J. Jeon, C.W. Ahn, Flexible transparent electrodes made of core-shell-structured carbon/metal hybrid nanofiber mesh films fabricated via electrospinning and electroplating, *Curr. Appl. Phys.* 17 (2017) 1401–1408.
- [65] H.S. Jo, S. An, J.-G. Lee, H.G. Park, S.S. Al-Deyab, A.L. Yarin, S.S. Yoon, Highly flexible, stretchable, patternable, transparent copper fiber heater on a complex 3D surface, *NPG Asia Mater.* 9 (2017) e347.
- [66] S. An, H.S. Jo, S.S. Al-Deyab, A.L. Yarin, S.S. Yoon, Nano-textured copper oxide nanofibers for efficient air cooling, *J. Appl. Phys.* 119 (2016), 065306.
- [67] S. An, H.S. Jo, D.Y. Kim, H.J. Lee, B.K. Ju, S.S. Al-Deyab, J.H. Ahn, Y. Qin, M. T. Swihart, A.L. Yarin, Self-junctioned copper nanofiber transparent flexible conducting film via electrospinning and electroplating, *Adv. Mater.* 28 (2016) 7149–7154.
- [68] S. Sinha-Ray, M.W. Lee, S. Sinha-Ray, S. An, B. Pourdeyehimi, S.S. Yoon, A. L. Yarin, Supersonic nanoblowing: a new ultra-stiff phase of nylon 6 in 20–50 nm confinement, *J. Mater. Chem. C* 1 (2013) 3491–3498.
- [69] S. An, C. Lee, M. Liou, H.S. Jo, J.-J. Park, A.L. Yarin, S.S. Yoon, Supersonically blown ultrathin thorny devil nanofibers for efficient air cooling, *ACS Appl. Mater. Interfaces* 6 (2014) 13657–13666.
- [70] B.S. Soram, I.S. Thangjam, J.Y. Dai, T. Kshetri, N.H. Kim, J.H. Lee, Flexible transparent supercapacitor with core-shell Cu@ Ni@ NiCoS nanofibers network electrode, *Chem. Eng. J.* 395 (2020), 125019.
- [71] R. Zhou, W. Guo, R. Yu, C. Pan, Highly flexible, conductive and catalytic Pt networks as transparent counter electrodes for wearable dye-sensitized solar cells, *J. Mater. Chem. A* 3 (2015) 23028–23034.
- [72] F. Reith, S.G. Campbell, A.S. Ball, A. Pring, G. Southam, Platinum in Earth surface environments, *Earth Sci. Rev.* 131 (2014) 1–21.
- [73] S. Xia, C. Wei, J. Tang, J. Yan, Tensile stress-gated electromagnetic interference shielding fabrics with real-time adjustable shielding efficiency, *ACS Sustain. Chem. Eng.* 9 (2021) 13999–14005.
- [74] Y. Chen, Z. Wang, R. Xu, W. Wang, D. Yu, A highly sensitive and wearable pressure sensor based on conductive polyacrylonitrile nanofibrous membrane via electroless silver plating, *Chem. Eng. J.* 394 (2020), 124960.
- [75] G.H. Kim, J.H. Shin, T. An, G. Lim, Junction-free flat copper nanofiber network-based transparent heater with high transparency, high conductivity, and high temperature, *Sci. Rep.* 8 (2018), 13581.
- [76] R. Song, X. Li, F. Gu, L. Fei, Q. Ma, Y. Chai, An ultra-long and low junction-resistance Ag transparent electrode by electrospun nanofibers, *RSC Adv.* 6 (2016) 91641–91648.
- [77] A. Testa, R. Bernasconi, R. Yoshikawa, I. Takenaka, L. Magagnin, S. Shiratori, Transparent flexible electrodes based on junctionless copper nanowire network via selective electroless metallization of electrospun nanofibers, *J. Electrochem. Soc.* 164 (2017) D764–D770.
- [78] T.Q. Aminu, D.F. Bahr, Control of copper nanoparticle metallization on electrospun fibers via Pd and Ag seed-assisted templating, *J. Mater. Sci.* 56 (2021) 16307–16323.
- [79] G.H. Kim, H. Woo, S. Kim, T. An, G. Lim, Highly-robust, solution-processed flexible transparent electrodes with a junction-free electrospun nanofiber network, *RSC Adv.* 10 (2020) 9940–9948.
- [80] J. Song, M.-R. Kim, Y. Kim, D. Seo, K. Ha, T.-E. Song, W.-G. Lee, Y. Lee, K.-C. Kim, C.W. Ahn, Fabrication of junction-free Cu nanowire networks via Ru-catalyzed electroless deposition and their application to transparent conducting electrodes, *Nanotechnology* 33 (2021), 065303.
- [81] S.Q. Jiang, C.W. Kan, C.W.M. Yuen, W.K. Wong, Electroless nickel plating of polyester fiber, *J. Appl. Polym. Sci.* 108 (2008) 2630–2637.
- [82] P. Schechner, E. Kroll, E. Bubis, S. Chervinsky, E. Zussman, Silver-plated electrospun fibrous anode for glucose alkaline fuel cells, *J. Electrochem. Soc.* 154 (2007), B942.
- [83] N.J. Pinto, P. Carrión, J.X. Quinones, Electroless deposition of nickel on electrospun fibers of 2-acrylamido-2-methyl-1-propanesulfonic acid doped polyaniline, *Mater. Sci. Eng. A* 366 (2004) 1–5.
- [84] R. Warren, C.H. Anderson, M. Carlsson, High-temperature compatibility of carbon fibres with nickel, *J. Mater. Sci.* 13 (1978) 178–188.
- [85] E. Hajjari, M. Divandari, A.R. Mirhabibi, The study of electroless coating of nickel on carbon fibers, *Iran. J. Mater. Sci. Eng.* 1 (2004) 3–48.
- [86] H. Liu, H. Gu, G. Li, N. Li, Fabrication of PAN/Ag/ZnO microporous membrane and examination of visible light photocatalytic performance, *Fibers Polym.* 22 (2021) 306–313.
- [87] R. Yadav, K. Balasubramanian, Metallization of electrospun PAN nanofibers via electroless gold plating, *RSC Adv.* 5 (2015) 24990–24996.
- [88] F. Muench, Electroless plating of metal nanomaterials, *ChemElectroChem* 8 (2021) 2993–3012.
- [89] P.-C. Hsu, D. Kong, S. Wang, H. Wang, A.J. Welch, H. Wu, Y. Cui, Electrolessly deposited electrospun metal nanowire transparent electrodes, *J. Am. Chem. Soc.* 136 (2014) 10593–10596.
- [90] G. Mondin, F.M. Wisser, A. Leifert, N. Mohamed-Noriega, J. Grothe, S. Dörfler, S. Kaskel, Metal deposition by electroless plating on polydopamine functionalized micro- and nanoparticles, *J. Colloid Interface Sci.* 411 (2013) 187–193.
- [91] Y. Fu, L. Liu, L. Zhang, W. Wang, Highly conductive one-dimensional nanofibers: silvered electrospun silica nanofibers via poly (dopamine) functionalization, *ACS Appl. Mater. Interfaces* 6 (2014) 5105–5112.
- [92] L. Miao, G. Liu, J. Wang, Ag-nanoparticle-bearing poly (vinylidene fluoride) nanofiber mats as janus filters for catalysis and separation, *ACS Appl. Mater. Interfaces* 11 (2019) 7397–7404.
- [93] M. Chung, W.H. Skinner, C. Robert, C.J. Campbell, R.M. Rossi, V. Koutsos, N. Radaesi, Fabrication of a wearable flexible sweat pH sensor based on SERS-active Au/TPU electrospun nanofibers, *ACS Appl. Mater. Interfaces* 13 (2021) 51504–51518.
- [94] Y.-K. Fuh, L.-C. Lien, Pattern transfer of aligned metal nano/microwires as flexible transparent electrodes using an electrospun nanofiber template, *Nanotechnology* 24 (2013), 055301.
- [95] P.-C. Hsu, S. Wang, H. Wu, V.K. Narasimhan, D. Kong, H. Ryoung Lee, Y. Cui, Performance enhancement of metal nanowire transparent conducting electrodes by mesoscale metal wires, *Nat. Commun.* 4 (2013), 2522.
- [96] P. Li, J. Ma, H. Xu, X. Xue, Y. Liu, Highly stable copper wire/alumina/polyimide composite films for stretchable and transparent heaters, *J. Mater. Chem. C* 4 (2016) 3581–3591.
- [97] J. Liang, Q. Liu, T. Li, Y. Luo, S. Lu, X. Shi, F. Zhang, A.M. Asiri, X. Sun, Magnetron sputtering enabled sustainable synthesis of nanomaterials for energy electrocatalysis, *Green Chem.* 23 (2021) 2834–2867.
- [98] M. Liu, P. Ren, H. Qiao, M. Zhang, W. Wu, B. Li, H. Wang, D. Luo, J. Liu, Y. Wang, High temperature-resistant transparent conductive films for photoelectrochemical devices based on W/Ag composite nanonetworks, *Nanomaterials* 13 (2023) 708.
- [99] Y. Meng, A. Liu, Z. Guo, G. Liu, B. Shin, Y.-Y. Noh, E. Fortunato, R. Martins, F. Shan, Electronic devices based on oxide thin films fabricated by fiber-to-film process, *ACS Appl. Mater. Interfaces* 10 (2018) 18057–18065.
- [100] T. Kerdcharoen, C. Wongchoosuk, Carbon nanotube and metal oxide hybrid materials for gas sensing, in: *Semiconductor Gas Sensors*, Elsevier, 2013, pp. 386–407.
- [101] R. Melentiev, A. Yudhanto, R. Tao, T. Vuchkov, G. Lubineau, Metallization of polymers and composites: State-of-the-art approaches, *Mater. Des.* 110958 (2022).
- [102] P.V. Maryin, A.Y. Fedotkin, E.N. Bolbasov, A.I. Kozelskaya, M.A. Buldakov, A. A. Evtina, N.V. Cherdynseva, S. Rutkowski, S.I. Tverdokhlebov, Surface modification of PLLA scaffolds via reactive magnetron sputtering in mixtures of nitrogen with noble gases for higher cell adhesion and proliferation, *Colloids Surf., A Physicochem. Eng. Asp.* 649 (2022), 129464.
- [103] J. Yang, C. Bao, K. Zhu, T. Yu, Q. Xu, High-performance transparent conducting metal network electrodes for perovskite photodetectors, *ACS Appl. Mater. Interfaces* 10 (2018) 1996–2003.
- [104] H. Nazari, G. Barati Darband, R. Arefinia, A review on electroless Ni-P nanocomposite coatings: effect of hard, soft, and synergistic nanoparticles, *J. Mater. Sci.* 58 (2023) 4292–4358.
- [105] C.-C. Lai, R. Boyd, P.-O. Svensson, C. Höglund, L. Robinson, J. Birch, R. Hall-Wilton, Effect of substrate roughness and material selection on the microstructure of sputtering deposited boron carbide thin films, *Surf. Coat. Technol.* 433 (2022), 128160.
- [106] N.B. Kiremitler, A. Esidir, Z. Gozutok, A.T. Ozdemir, M.S. Onses, Rapid fabrication of high-performance transparent electrodes by electrospinning of reactive silver ink containing nanofibers, *J. Ind. Eng. Chem.* 95 (2021) 109–119.
- [107] W. Li, T. Bai, G. Fu, Q. Zhang, J. Liu, H. Wang, Y. Sun, H. Yan, Progress and challenges in flexible electrochromic devices, *Sol. Energy Mater. Sol. Cells* 240 (2022), 111709.
- [108] D.-H. Jiang, P.-C. Tsai, C.-C. Kuo, F.-C. Jhuang, H.-C. Guo, S.-P. Chen, Y.-C. Liao, T. Satoh, S.-H. Tung, Facile preparation of Cu/Ag core/shell electrospun nanofibers as highly stable and flexible transparent conducting electrodes for optoelectronic devices, *ACS Appl. Mater. Interfaces* 11 (2019) 10118–10127.
- [109] M.J. Nikzad, N. Mohamadbeigi, S.K. Sadrnezhaad, S.M. Mahdavi, Fabrication of a highly flexible and affordable transparent electrode by aligned u-shaped copper nanowires using a new electrospinning collector with convenient transferability, *ACS Omega* 4 (2019) 21260–21266.
- [110] S.B. Singh, Y. Hu, T. Kshetri, N.H. Kim, J.H. Lee, An embedded-PVA@ Ag nanofiber network for ultra-smooth, high performance transparent conducting electrodes, *J. Mater. Chem. C* 5 (2017) 4198–4205.
- [111] Y. Wang, Y. Xu, D. Wang, Y. Zhang, X. Zhang, J. Liu, Y. Zhao, C. Huang, X. Jin, Polytetrafluoroethylene/polyphenylene sulfide needle-punched triboelectric air filter for efficient particulate matter removal, *ACS Appl. Mater. Interfaces* 11 (2019) 48437–48449.
- [112] W. Zhong, Y. Li, Q. Zhang, C. Chang, F. Wang, J. Xiao, Junction-free copper wires with submicron linewidth for large-area high-performance transparent electrodes, *J. Mater. Chem. C* 7 (2019) 6144–6151.
- [113] S.J. Kim, T.H. Phung, S. Kim, M.K. Rahman, K.S. Kwon, Low-cost fabrication method for thin, flexible, and transparent touch screen sensors, *Adv. Mater. Technol.* 5 (2020), 2000441.
- [114] C. Bao, J. Yang, H. Gao, F. Li, Y. Yao, B. Yang, G. Fu, X. Zhou, T. Yu, Y. Qin, In situ fabrication of highly conductive metal nanowire networks with high transmittance from deep-ultraviolet to near-infrared, *ACS Nano* 9 (2015) 2502–2509.
- [115] X. Wang, Y. Zhang, X. Zhang, Z. Huo, X. Li, M. Que, Z. Peng, H. Wang, C. Pan, A highly stretchable transparent self-powered triboelectric tactile sensor with metallized nanofibers for wearable electronics, *Adv. Mater.* 30 (2018), 1706738.
- [116] Z.L. Wang, From contact electrification to triboelectric nanogenerators, *Rep. Prog. Phys.* 84 (2021), 096502.

- [117] J. Park, B.G. Hyun, B.W. An, H.-G. Im, Y.-G. Park, J. Jang, J.-U. Park, B.-S. Bae, Flexible transparent conductive films with high performance and reliability using hybrid structures of continuous metal nanofiber networks for flexible optoelectronics, *ACS Appl. Mater. Interfaces* 9 (2017) 20299–20305.
- [118] J. Choi, Y.S. Shim, C.H. Park, H. Hwang, J.H. Kwack, D.J. Lee, Y.W. Park, B.K. Ju, Junction-free electrospun Ag fiber electrodes for flexible organic light-emitting diodes, *Small* 14 (2018), 1702567.
- [119] J. Zhao, Z. Chi, Z. Yang, X. Chen, M.S. Arnold, Y. Zhang, J. Xu, Z. Chi, M. P. Aldred, Recent developments of truly stretchable thin film electronic and optoelectronic devices, *Nanoscale* 10 (2018) 5764–5792.
- [120] J. Kim, B. Kim, J. Eun, B.-J. Yoon, S. Jeon, Y.S. Do, S.-H. Jeong, A concept of stretchable coaxial cable based on one-body Au nanonetworks, *J. Ind. Eng. Chem.* 124 (2023) 455–461.
- [121] I.C. Ciobotaru, M. Enculescu, S. Polosan, I. Enculescu, C.C. Ciobotaru, Organic light-emitting diodes with electrospun electrodes for double-side emissions, *Micromachines* 14 (2023), 543.
- [122] H.M. Lee, M.H. Kim, Y. Jin, Y. Jang, P.S. Lee, S.-H. Jeong, Hierarchically engineered unibody Au mesh for stretchable and transparent conductors, *J. Mater. Chem. A* 11 (2023) 4220–4229.
- [123] J. Lee, S. Varagnolo, M. Walker, R.A. Hatton, Transparent fused nanowire electrodes by condensation coefficient modulation, *Adv. Funct. Mater.* 30 (2020), 2005959.
- [124] B.W. An, E.-J. Gwak, K. Kim, Y.-C. Kim, J. Jang, J.-Y. Kim, J.-U. Park, Stretchable, transparent electrodes as wearable heaters using nanotrough networks of metallic glasses with superior mechanical properties and thermal stability, *Nano Lett.* 16 (2016) 471–478.
- [125] J. Jang, B.G. Hyun, S. Ji, E. Cho, B.W. An, W.H. Cheong, J.-U. Park, Rapid production of large-area, transparent and stretchable electrodes using metal nanofibers as wirelessly operated wearable heaters, *NPG Asia Mater.* 9 (2017), e432.
- [126] J.-H. Lee, D.-Y. Youn, Z. Luo, J.Y. Moon, S.-J. Choi, C. Kim, I.-D. Kim, Cu microbelt network embedded in colorless polyimide substrate: flexible heater platform with high optical transparency and superior mechanical stability, *ACS Appl. Mater. Interfaces* 9 (2017) 39650–39656.
- [127] K. Hong, J. Ham, B.-J. Kim, J.Y. Park, D.C. Lim, J.Y. Lee, J.-L. Lee, Continuous 1D-metallic microfibers web for flexible organic solar cells, *ACS Appl. Mater. Interfaces* 7 (2015) 27397–27404.
- [128] J. Kim, J. Kang, U. Jeong, H. Kim, H. Lee, Catalytic, conductive, and transparent platinum nanofiber webs for FTO-free dye-sensitized solar cells, *ACS Appl. Mater. Interfaces* 5 (2013) 3176–3181.
- [129] S.B. Singh, T.I. Singh, N.H. Kim, J.H. Lee, A core-shell MnO₂@ Au nanofiber network as a high-performance flexible transparent supercapacitor electrode, *J. Mater. Chem. A* 7 (2019) 10672–10683.
- [130] S. Lee, S.-W. Kim, M. Ghidelli, H.S. An, J. Jang, A.L. Bassi, S.-Y. Lee, J.-U. Park, Integration of transparent supercapacitors and electrodes using nanostructured metallic glass films for wirelessly rechargeable, skin heat patches, *Nano Lett.* 20 (2020) 4872–4881.
- [131] S.B. Singh, T. Kshetri, T.I. Singh, N.H. Kim, J.H. Lee, Embedded PEDOT: PSS/AgNFs network flexible transparent electrode for solid-state supercapacitor, *Chem. Eng. J.* 359 (2019) 197–207.
- [132] S.B. Singh, D.T. Tran, K.U. Jeong, N.H. Kim, J.H. Lee, A flexible and transparent zinc-nanofiber network electrode for wearable electrochromic, rechargeable Zn-Ion battery, *Small* 18 (2022), 2104462.
- [133] A. Miyamoto, S. Lee, N.F. Cooray, S. Lee, M. Mori, N. Matsuhisa, H. Jin, L. Yoda, T. Yokota, A. Itoh, M. Sekino, H. Kawasaki, T. Ebihara, M. Amagai, T. Someya, Inflammation-free, gas-permeable, lightweight, stretchable on-skin electronics with nanomeshes, *Nat. Nanotechnol.* 12 (2017) 907–913.
- [134] M. Ren, J. Li, L. Lv, M. Zhang, X. Yang, Q. Zhou, D. Wang, R. Dhakal, Z. Yao, Y. Li, A wearable and high-performance capacitive pressure sensor based on a biocompatible PVP nanofiber membrane via electrospinning and UV treatment, *J. Mater. Chem. C* 10 (2022) 10491–10499.
- [135] O. Yue, X. Wang, X. Liu, M. Hou, M. Zheng, Y. Wang, B. Cui, Spider-web and ant-tentacle doubly bio-inspired multifunctional self-powered electronic skin with hierarchical nanostructure, *Adv. Sci.* 8 (2021), 2004377.
- [136] H. Tabasum, N. Gill, R. Mishra, S. Lone, Wearable microfluidic-based e-skin sweat sensors, *RSC Adv.* 12 (2022) 8691–8707.
- [137] R. Dahiya, D. Akinwande, J.S. Chang, Flexible electronic skin: From humanoids to humans [scanning the issue], *Proc. IEEE* 107 (2019) 2011–2015.
- [138] X. Peng, K. Dong, C. Ning, R. Cheng, J. Yi, Y. Zhang, F. Sheng, Z. Wu, Z.L. Wang, All-nanofiber self-powered skin-interfaced real-time respiratory monitoring system for obstructive sleep apnea-hypopnea syndrome diagnosing, *Adv. Funct. Mater.* 31 (2021), 2103559.
- [139] Z. Ma, Q. Huang, Q. Xu, Q. Zhuang, X. Zhao, Y. Yang, H. Qiu, Z. Yang, C. Wang, Y. Chai, Permeable superelastic liquid-metal fibre mat enables biocompatible and monolithic stretchable electronics, *Nat. Mater.* 20 (2021) 859–868.
- [140] J. Dong, Y. Peng, L. Pu, K. Chang, L. Li, C. Zhang, P. Ma, Y. Huang, T. Liu, Perspiration-wicking and luminescent on-skin electronics based on ultrastretchable Janus E-textiles, *Nano Lett.* 22 (2022) 7597–7605.
- [141] M. Wang, C. Ma, P.C. Uzabakirho, X. Chen, Z. Chen, Y. Cheng, Z. Wang, G. Zhao, Stencil printing of liquid metal upon electrospun nanofibers enables high-performance flexible electronics, *ACS Nano* 15 (2021) 19364–19376.
- [142] S. Wei, R. Yin, T. Tang, Y. Wu, Y. Liu, P. Wang, K. Wang, M. Mei, R. Zou, X. Duan, Gas-permeable, irritation-free, transparent hydrogel contact lens devices with metal-coated nanofiber mesh for eye interfacing, *ACS Nano* 13 (2019) 7920–7929.
- [143] T. He, A. Xie, D.H. Reneker, Y. Zhu, A tough and high-performance transparent electrode from a scalable and transfer-free method, *ACS Nano* 8 (2014) 4782–4789.
- [144] S. An, H.S. Jo, Y.I. Kim, K.Y. Song, M.-W. Kim, K.B. Lee, A.L. Yarin, S.S. Yoon, Bio-inspired, colorful, flexible, defrostable light-scattering hybrid films for the effective distribution of LED light, *Nanoscale* 9 (2017) 9139–9147.